iScience

CellPress
OPEN ACCESS

Article

The genome of a hadal sea cucumber reveals novel adaptive strategies to deep-sea environments

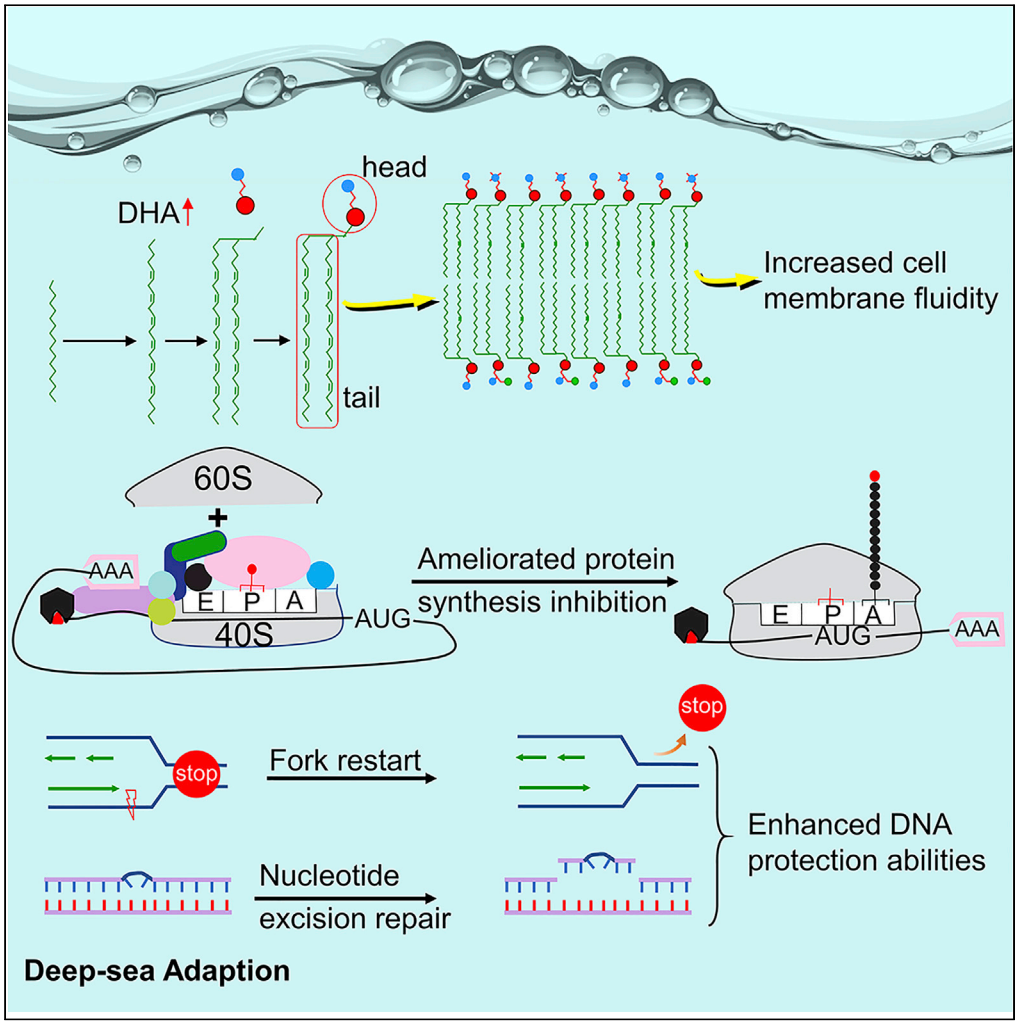

Guangming Shao, Tianliang He, Yinnan Mu, ..., Dinggao Liu, Liangsheng Zhang, Xinhua Chen

fafuzhang@163.com (L.Z.)
chenxinhua@tio.org.cn (X.C.)

Highlights

The genome of hadal sea cucumber *Paelopatides* sp. Yap was sequenced and characterized

Altering the content of DHA and phosphatidylethanolamine is a way to deep-sea adaptation

Paelopatides sp. Yap enhanced DNA protection abilities for high-pressure adaptation

Paelopatides sp. Yap evolved to ameliorate protein synthesis inhibition in the hadal zone

Shao et al., iScience *25*, 105545
December 22, 2022
https://doi.org/10.1016/j.isci.2022.105545

iScience

CellPress
OPEN ACCESS

Article

The genome of a hadal sea cucumber reveals novel adaptive strategies to deep-sea environments

Guangming Shao,[1] Tianliang He,[1] Yinnan Mu,[1] Pengfei Mu,[1] Jingqun Ao,[1] Xihuang Lin,[2] Lingwei Ruan,[2] YuGuang Wang,[2] Yuan Gao,[4] Dinggao Liu,[4] Liangsheng Zhang,[4,*] and Xinhua Chen[1,3,5,*]

SUMMARY

How organisms cope with coldness and high pressure in the hadal zone remains poorly understood. Here, we sequenced and assembled the genome of hadal sea cucumber *Paelopatides* sp. Yap with high quality and explored its potential mechanisms for deep-sea adaptation. First, the expansion of *ACOX1* for rate-limiting enzyme in the DHA synthesis pathway, increased DHA content in the phospholipid bilayer, and positive selection of *EPT1* may maintain cell membrane fluidity. Second, three genes for translation initiation factors and two for ribosomal proteins underwent expansion, and three ribosomal protein genes were positively selected, which may ameliorate the protein synthesis inhibition or ribosome dissociation in the hadal zone. Third, expansion and positive selection of genes associated with stalled replication fork recovery and DNA repair suggest improvements in DNA protection. This is the first genome sequence of a hadal invertebrate. Our results provide insights into the genetic adaptations used by invertebrate in deep oceans.

INTRODUCTION

The hadal zone lies at the bottom of the deepest oceanic trenches at depths of 6,000-11,000 m. This deep-sea environment is characterized by food shortage, darkness, hypoxia, low temperature, and high hydrostatic pressure.[1] Hydrostatic pressure, which increases by approximately one atmosphere for every 10 m increment in-depth, strongly constrains the vertical distribution of marine organisms. The effects of high hydrostatic pressure on cell physiology are pleiotropic and primarily include reduction in cell membrane fluidity,[2,3] inhibition of protein synthesis,[4,5] and replication fork stalling and DNA damage.[6–9] Low temperature has similar inhibitory effects on cell membrane fluidity[10] and protein synthesis.[11,12] Nevertheless, many diverse groups of organisms survive and thrive in the hadal zone.[1,13,14] However, the adaptive mechanisms of these organisms for the hadal environment were poorly understood. Recently, two genomes of the hadal snailfish from the Mariana Trench and Yap Trench were reported, and pressure-tolerant cartilage, enhanced cell membrane fluidity and transport protein activity, increased protein stability and DNA repair have been suggested to be associated with hadal adaption,[15,16] which provided paradigms for genetic adaptation to the hadal environment. Nevertheless, due to a lack of genomic data for hadal species, it remains largely unclear how these organisms cope with their hostile hadal environment.

The Yap Trench lies in the western Pacific Ocean and neighbors the Mariana Trench. In June 2017, three sea cucumbers were collected in the Yap Trench using the Jiaolong Manned Submarine at depths of 5,090 m, 6,429 m, and 6,633 m and at 1.49-1.71°C (Figure 1A and Table S1). These specimens were preliminarily designated "Yap hadal sea cucumbers" (YHSCs). In this study, we sequenced and characterized the genome of a YHSC collected at 6,633 m. We then explored the strategies employed by YHSCs for deep-sea adaption.

RESULTS AND DISCUSSIONS

Yap hadal sea cucumbers genome characteristics

In this study, approximately 209.1 Gb Illumina clean reads were produced from genome sequencing and used to estimate the genomic characteristics. The estimated size is 3.54 Gb with a repeat content of 73.93% and a heterozygosity rate of 2.9% (Figure S1, and Table S2). Then, PacBio sequencing generated 490.9 Gb subreads (Table S3), with a depth of 133×. These subreads were assembled into 59,054 contigs,

[1]Key Laboratory of Marine Biotechnology of Fujian Province, Institute of Oceanology, College of Marine Sciences, Fujian Agriculture and Forestry University, Fuzhou, Fujian 350002, China

[2]Key Laboratory of Marine Biogenetic Resources, Third Institute of Oceanography, Ministry of Natural Resources, Xiamen, Fujian 361005, China

[3]Southern Marine Science and Engineering Guangdong Laboratory (Zhuhai), Zhuhai, Guangdong 519000, China

[4]Genomics and Genetic Engineering Laboratory of Ornamental Plants, College of Agriculture and Biotechnology, Zhejiang University, Hangzhou 310058, China

[5]Lead contact

*Correspondence: fafuzhang@163.com (L.Z.), chenxinhua@tio.org.cn (X.C.)

https://doi.org/10.1016/j.isci.2022.105545

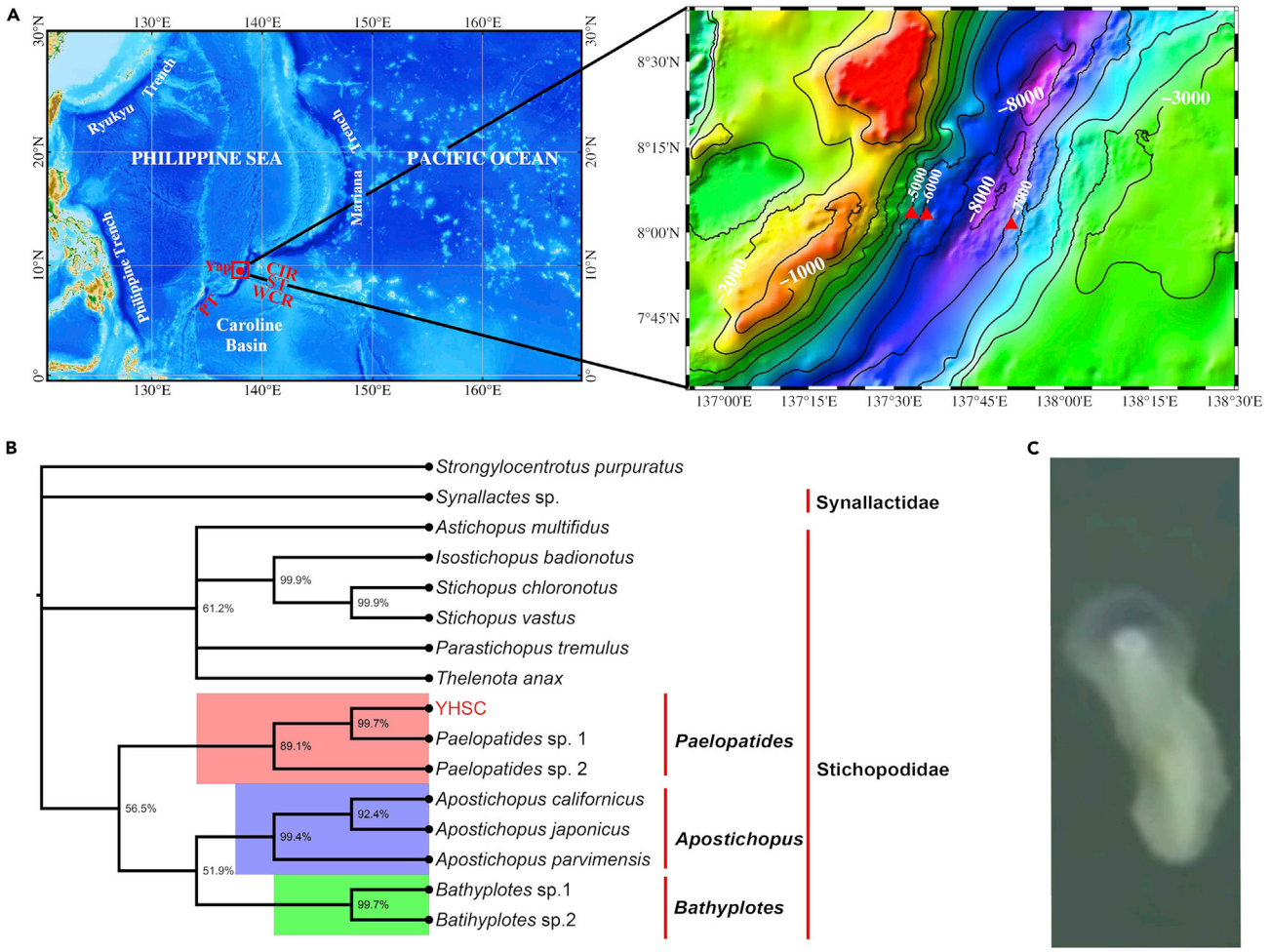

Figure 1. YHSC capture locations, phylogenetic position, and morphology

(A) Location of the Yap Trench (left) and the sampling points (▲) on a bathymetric map (right). YAP: Yap Trench; CIR: Caroline Islands Ridge; ST: Sorol Trough; WCR: West Caroline Rise; and PT: Palau Trench.

(B) Bayesian inference tree based on three concatenated nuclear genes: *18S rRNA*, *28S rRNA*, and *H3*. The numbers at nodes represent the bootstrap scores.

(C) Gross morphology of YHSC.

of which 2740 were identified as redundant sequences and excluded. GC depth scatterplots were used to evaluate the contamination in the sequencing data. No interruptions were detected along the horizontal axis of the GC-depth scatterplot, indicating no obvious sample contamination (Figure S2). Nevertheless, 876 contigs were identified as bacterial contamination and were ruled out (Table S4). The final genome consists of 55,447 contigs with a total size of 3.70 Gb and an N50 of 137.1 kb (Table S5). The small gap between the estimated size and final size can result from low estimation accuracy, considering the serious effects of repeats and high heterozygosity on the accuracy of genome size estimation.[17,18] Additionally, it took more than 3 h for the submarine to bring the specimens from the sampling site to the mothership, during which the specimens suffered a high level of DNA damage. The peak size of the DNA sample is only 15,860 bp and the DNA integrity number (DIN) is 6.7 (Figure S3). The DNA damage is mainly caused by rapid and prolonged decompression stress during specimen collection as previously indicated,[7] which prevented us from further assembling the contigs into scaffolds by conducting Hi-C,[19] Chicago[20] or Bionano.[21] Read mapping rate is an important metric assessing the completeness of assembly.[22,23] In this study, approximately 99.11% of the Illumina reads were successfully mapped to the polished contigs, reflecting the completeness of the YHSC genome assembly (Table S6). We identified 89.4% complete benchmarking universal single-copy orthologs (BUSCOs) in the genome assembly (Table S7), again reflecting high genome integrity. In addition, 57,522 genes were successfully annotated using a combination of homology-based predictions, *ab initio* gene prediction, and transcript evidence in YHSC (Table S8).

Phylogenetic position and evolutionary history of the Yap hadal sea cucumbers

Blastn searches against the NCBI nt database indicated that the nucleic acid sequences of two mitochondrial genes—16S rRNA gene (*16S rRNA*) and cytochrome oxidase subunit I (*COI*), and three nuclear genes—18S rRNA gene (*18S rRNA*), 28S rRNA gene (*28S rRNA*) and histone H3 (*H3*) from the YHSC were most similar to the corresponding genes from the deep-sea holothurian *Paelopatides* sp. 1.[24] Multigene phylogenies of the extant Holothuroidea based on the three nuclear genes or the two mitochondrial genes (Table S9) showed that the YHSC formed a clade with *Paelopatides* sp. 1 and *Paelopatides* sp. 2, suggesting that the YHSC may fall into this genus (Figures 1B, S4A-S4B). To test this possibility, we calculated the genetic divergence between the YHSC and seven closely related species in *Paelopatides*, *Bathyplotes*, and *Apostichopus* based on the *COI* barcoding gene (Table S10). Across all seven comparisons, only the genetic distance between the YHSC and *Paelopatides* sp. 1 (1.05) and the genetic distance between the YHSC and *Paelopatides* sp. 2 (11.87) were within the range typical of congeneric divergences in Holothuroidea (2.16-17.02; mean: 12.41).[25] Thus, we hypothesize that the YHSC falls into the Paelopatides rather than the *Bathyplotes* or *Apostichopus*. In all *phylogenies*, *Paelopatides*, *Bathyplotes*, and *Apostichopus* formed a clade corresponding to Stichopodidae (Figures 1B, S4A-S4B), consistent with the transfer of Paelopatides and *Bathyplotes* to Stichopodidae in the recent revision.[24] However, it should be noted that the assignment of the YHSC to Paelopatides within Stichopodidae remains tentative. For one thing, the molecular data of many other genera in Stichopodidae except for those mentioned above is still lacking; for another, the monophyly of Paelopatides has not been confirmed, and the morphology of *Paelopatides* sp. 1, *Paelopatides* sp. 2, and YHSC has not been checked.

In appearance, the YHSC is sub-cylindrical. Except for a small area at one end, the whole body of YHSC is translucent white (Figure 1C and Video S1). Dated phylogenetic trees of Holothuroidea based on different calibration points are highly incongruent.[24] However, the two possible divergence times between Apostichopus and *Paelopatides* have been estimated to be 74 or 91 million years ago (Ma),[24] which substantially predated the formation of the Yap Trench (40 Ma).[26–29] This suggested that the YHSC diverged from *Apostichopus japonicus* before colonizing the hadal zone.

Inference of whole genome duplication

In the consideration of the high gene number in the YHSC genome, whole genome duplications (WGDs) were inferred from *Ks* age distribution. The whole paranome *Ks* distributions for both *A. japonicus* and YHSC are typically L-shaped until at least the *Ks* peak of their orthologs (Figure S5), indicating that YHSC didn't experience any WGDs after its differentiation with *A. japonicus* according to previous interpretation.[30,31] Thus, YHSC should be diploid, given that *A. japonicus* has a diploid genome.[32,33]

Comparative genomics

We used CAFÉ (4.2)[34,35] to characterize the expansion and contraction of gene families in the YHSC genome compared with six other invertebrate genomes: *Drosophila melanogaster*, *Saccoglossus kowalevskii*, *Strongylocentrotus purpuratus*, *A. japonicus*, and two geographically separated populations of *Acanthaster planci* (Okinawa, Japan, and the Great Barrier Reef, Australia).[36] A total of 6030 and 2730 gene families are significantly expanded and contracted in the YHSC genome, respectively (Figure S6A). Thus, the gain-to-loss ratio of gene families is 2.2 (6030/2730). Comparisons of pfam functional domains among the seven invertebrate genomes suggested that the YHSC has the highest percentage of unique domains (Figure S6B). We identified 173 expanded domains in the YHSC genome (Table S11). The cutoff for expanded domains can be found in the quantification and statistical analysis section. These expanded domains were associated with many important biological processes, including transposons, genetic information processing, immunity, material transport, apoptosis, metabolism, and DNA binding (Figure S7).

Although it is routine that the identification and masking of repeats are performed before the gene prediction, repeat identification tools available at present can not totally find and mask all the repeats.[37] This is exactly the case for the YHSC genome with a high proportion of repeats. In this study, 24 of the 173 expanded domains exist in transposon-encoded proteins (Table S11). Although this proportion is low, the 24 expanded domains are involved in 9104 YHSC genes, accounting for 62.5% of the YHSC genes that contain at least one of the 173 expanded domains (14,578). Thus, increased gene number in the YHSC genome (57,522) compared with other echinoderm genomes (30,250 genes for *A. japonicus*, 24,743 genes for *A. planci*, 28,886 genes for *S. purpuratus*) mainly resulted from partial identification and incomplete masking of transposons during gene identification.

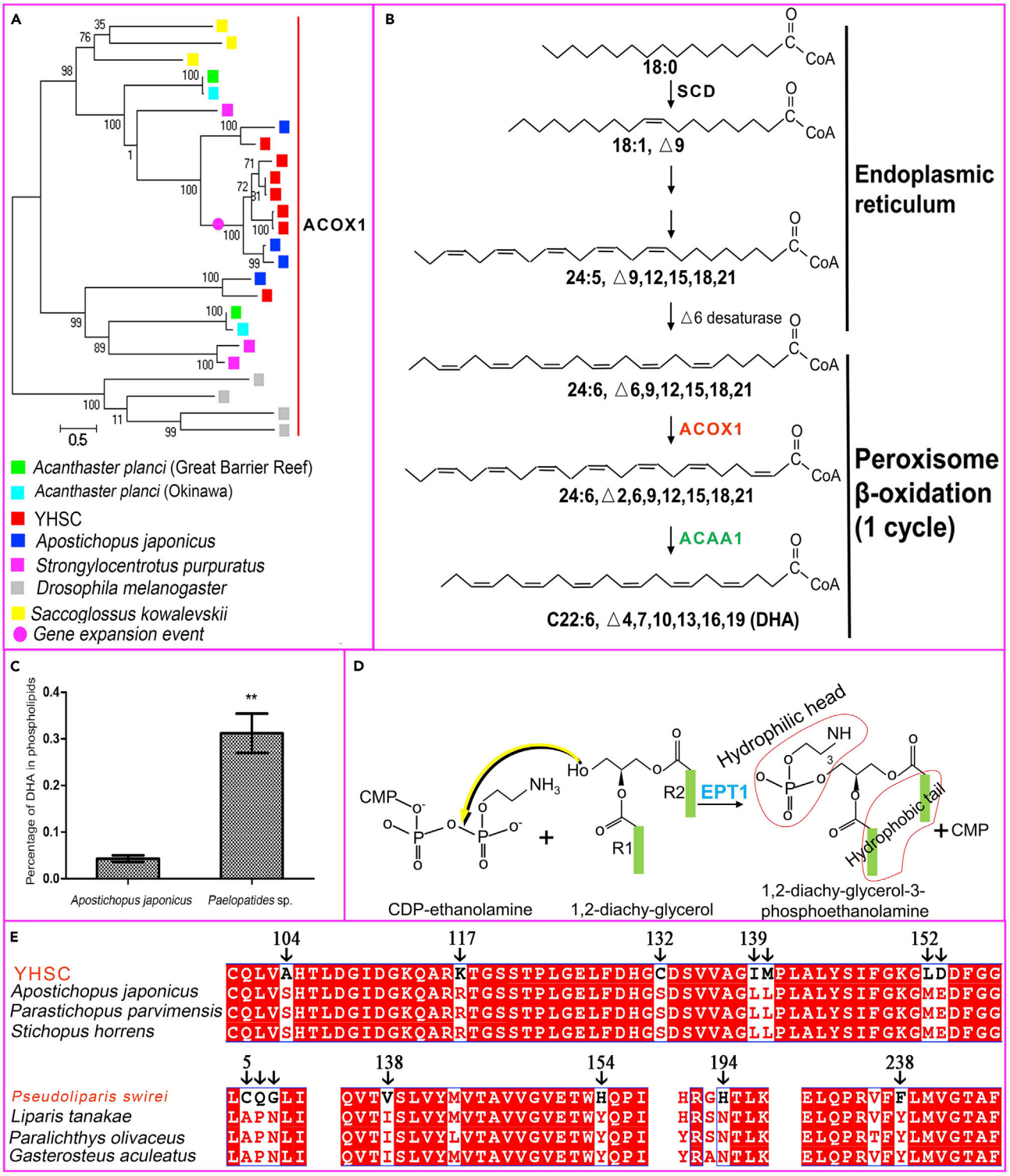

Figure 2. The adaptive evolution of phospholipids in the cell membrane in the hadal environment

(A) Phylogenetic tree constructed by FastTree (version 2.1.11) using the Jones-Taylor-Thorton (JTT) model of amino acid evolution based on protein sequences containing acyl-coenzyme A oxidase N-terminal (Acyl-CoA_ox_N) show that *ACOX1* genes, encoding the rate-limiting enzyme in the DHA synthesis pathway, expanded in the YHSC genome.

Figure 2. *Continued*

(B) DHA synthesis pathway. The *ACOX1* in red refers to expansion in the YHSC genome, while the *ACAA1* in green, encoding another rate-limiting enzyme, underwent expansion in the hadal snailfish *P. swirei*.[16]

(C) DHA content in phospholipids from *A. japonicus* and the YHSC. **, $p < 0.01$ (Student's t test) Statistical details can be found in the quantification and statistical analysis section.

(D) The production of phosphatidylethanolamine (one of the most abundant components of the cell membrane) catalyzed by EPT1. *EPT1* is a gene that experienced convergent evolution between the YHSC and *P. swirei*.

(E) Multiple sequence alignment of EPT1. Amino acids unique to the YHSC or *P. swirei* are indicated by arrows.

Convergent sequence evolution between the Yap hadal sea cucumbers and *Pseudoliparis swirei*

To determine whether convergent evolution occurs between YHSC and the hadal snailfish *P. swirei*,[16] we identified and compared their positively selected genes (PSGs). Positive selection analysis using the site-branch model in codeml identified 441 PSGs in the YHSC genome taking three closely related shallow-sea species of Holothuroidea (*Parastichopus parvimensis*, *Stichopus horrens,* and *A. japonicus*) as background branches. We also identified 397 PSGs in *P. swirei* using three shallow-sea fishes (*Paralichthys olivaceus*, *Gasterosteus aculeatus*, and *Liparis tanakae*) as background branches. Six PSGs were shared by the YHSC and *P. swirei*: ethanolamine phosphotransferase 1 (*EPT1*), nucleoporin 43 (*NUP*43), sorting nexin-17 (*SNX17*), mitochondrial ribosomal protein S27 (*MRPS27*), alpha-1,3- mannosyltransferase (*ALG3*), and XPC complex subunit, DNA damage recognition and repair factor (*XPC*), which are involved in the synthesis of phosphoethanolamine[38] (one of the most abundant phospholipids in cell membranes), mitosis and assembly of the nuclear pore complex,[39] sorting of low-density lipoprotein receptor-related protein 1,[40] mitochondrial ribosome, protein glycosylation,[41] and DNA repair,[42] respectively (Table S12). Due to the distant genetic relationships, no overlapping amino acid sites in the six PSGs between YHSC and *P. swirei* were identified. Nevertheless, these six genes were also considered to have experienced convergent positive selection since they evolved under selection in both organisms, even though their sequences have not converged at the amino acid level. Interestingly, most pathways or components in which these convergent genes are involved, such as cell membrane fluidity, mitosis, ribosome, and DNA repair, are destroyed by high pressure and low temperature in the hadal zone.

Repeat expansion in the Yap hadal sea cucumbers genome

Compared with the genomes of *A. japonicus*, *S. purpuratus,* and *A. planci*, the YHSC genome is highly repetitive. Approximately 76.06% of the YHSC genome namely 2.82 Gb was repeats, far exceeding those of the other echinoderm genomes (28.36-48.43%, 0.11-0.45Gb, Table S13). Thus, repeats drove the large-scale genome expansions in YHSC. The main type of the increased repeats in the YHSC genome is transposons, which occupies 58.82% of the YHSC genome, while the corresponding proportion is only 24.43-29.53% for other echinoderm genomes (Table S13). Except DNA transposon, the relative abundances of retroelements, rolling circles and unclassified types in the YHSC genome (16.19%, 2.13 and 38.49%, respectively) are far beyond those of the other genomes (2.93%-5.61%, 0-0.07%, and 14.82-24.15% respectively; Table S13). Among the retroelements identified, the most striking difference between YHSC and the other genomes was the proportion of Gypsy/DIRS1: which accounts for 7.90% of the YHSC genome, a percentage over ten times that of the other genomes (0.30-0.69%; Table S13). Additionally, other retroelements including Penelope, L2/CR1/Rex, RTE/Bov-B, and Retroviral also showed an expansion in the YHSC genome (Table S13). Although the significance of transposable elements in deep-sea adaptation is unknown, transposable elements are considered powerful drivers of genome evolution and phenotypic diversity by introducing genetic changes of great magnitude and variety.[43]

The expansion of the *ACOX1* gene for rate-limiting enzyme in the DHA synthesis pathway, the corresponding increase in DHA levels in phospholipids in the Yap hadal sea cucumbers, and the positive selection of the *EPT1* gene increased cell membrane fluidity

Fluidity is a fundamental feature of cell membranes and is vital for the execution of various physiological functions. However, both high hydrostatic pressure and low temperature, which are characteristic of the hadal zone, decrease biomembrane fluidity and the ease of phase transitions.[44,45] Double bonds in the fatty acid hydrocarbon chain, which constitute the hydrophobic tails of the phospholipid bilayer, can disorder the lipid bilayer and lower the phase-transition temperature.[3] (4Z,7Z,10Z,13Z,16Z,19Z)-docosa-4,7,10,13,16,19-hexaenoic acid (DHA, C22:6) has six double bonds and thus can drastically increase cell membrane fluidity.[46] In the YHSC genome, acyl-CoA oxidase 1 (*ACOX1*), a gene encoding rate-limiting enzymes in the DHA synthesis pathway was expanded (Figure 2A). The ACOX1 participates in the first step of

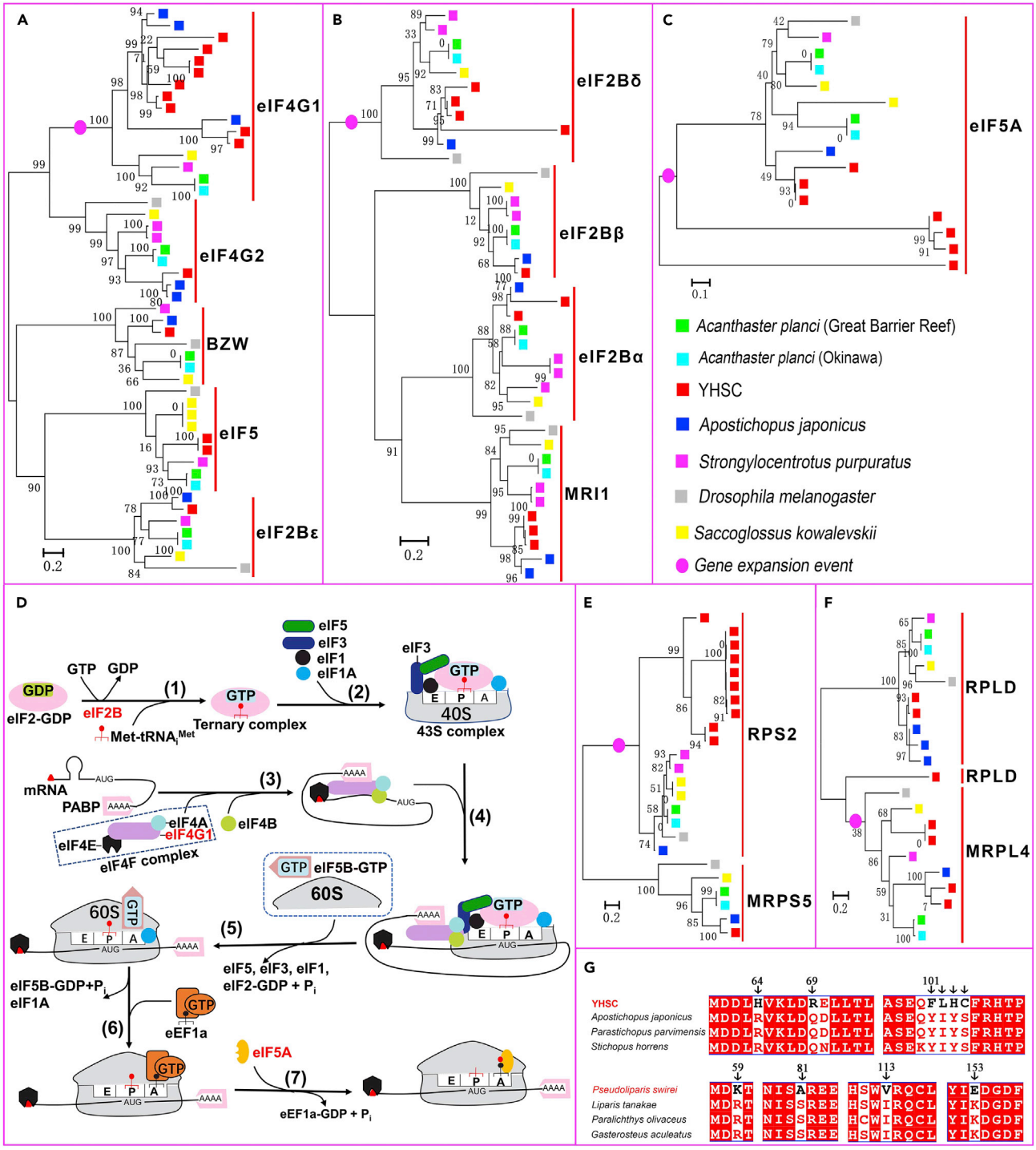

Figure 3. Adaptive changes in translation initiation factors and ribosomal proteins to combat protein synthesis inhibition induced by high pressure and low temperature in the hadal zone

(A–C) Phylogenetic trees showing the expansion of genes for the translation initiation factors *eIF4G1*, *eIF2Bδ*, and *eIF5A* in the YHSC genome.

(D) Model of the translation initiation pathways.[57–60] Expanded genes are marked in red. (1) eIF2B promotes the exchange of GDP-GTP on eIF2, a rate-limiting step of translation initiation. Then, eIF2-GTP forms a ternary complex (eIF2-GTP-Met-tRNA$_i^{Met}$) together with initiator tRNA (Met-tRNA$_i^{Met}$). (2) The ternary complex was recruited to 40S subunits to form 43S complexes with other factors. (3) The eIF4F complex, consisting of eIF4E, eIF4A, and eIF4G1, bound to mRNA and mediated the unwinding of the mRNA cap-proximal region with the help of eIF4B, and mRNA was activated. (4) 43S complex attached

Figure 3. *Continued*

to the activated mRNA and scans the 5′UTR of mRNA to the initiation codon - AUG. (5) eIF5B-mediated ribosomal subunits joining and displacement of translation initiation factors. (6) eEF1A carries aminoacyl-tRNA to the A site of the ribosome.[61] (7) eIF5A mediated the formation of the first peptide bond.[59,62]

(E and F) Phylogenetic trees based on protein sequences containing domains of Ribosomal_S5 (E), and Ribosomal_L4 (F) show the expansion of *RPS2* and *MRPL4* genes in the YHSC genome.

(G) Alignment of the amino acid sequence of MRPS27. *MRPS27* is a gene that experienced convergent positive selection between the YHSC and *P. swirei*. Amino acids unique to the YHSC or *P. swirei* are indicated by arrows.

β-oxidation in peroxisomes and functions by introducing a *trans* double bond into acyl chains[47,48] (Figure 2B). We identified seven copies of the *ACOX1* gene in the YHSC genome and no more than four copies in any of the other genomes examined (Figure 2A). Interestingly, the acetyl-CoA acyltransferase 1 (*ACAA1*) gene, encoding another rate-limiting enzyme and mediating the last step of DHA synthesis (Figure 2B), expanded in hadal *P. swirei*.[16] The expansion of the *ACOX1* gene in the YHSC genome and the *ACAA1* gene in hadal *P. swirei* may accelerate DHA synthesis to counteract the reduction in membrane fluidity associated with the high hydrostatic pressure and low temperature in the hadal zone, and strengthened DHA synthesis represents convergent evolution in the hadal YHSC and *P. swirei*.

We analyzed and compared the composition of fatty acids (C6-C24) in the phospholipid bilayer of the YHSC and *A. japonicus* and found that the relative abundances of four fatty acids differed significantly between the two species: tetradecanoic acid (C14:0), hexadecanoic acid (C16:0), heptadecanoic acid (C17:0), and DHA (Table S14). The fatty acid that differed most substantially between the two species was DHA; DHA content in the YHSC was approximately 7.3 times greater than that in *A. japonicus* (Figure 2C). This was consistent with the expansion of the *ACOX1* gene that encodes the rate-limiting enzyme in the DHA synthesis pathway in the YHSC genome. This suggested that over evolutionary time, the *ACOX1* gene encoding the rate-limiting enzyme in the DHA synthesis pathway multiplied in the YHSC genome, increasing DHA content in the phospholipid bilayer to maintain cell membrane fluidity under low temperature and high hydrostatic pressure.

Phospholipids alter membrane fluidity not only via their hydrophobic tails but also via their hydrophilic heads. Phosphatidylethanolamine, which constitutes over half of the total phospholipids in eukaryotic cell membranes[38] together with phosphatidylcholine, tends to reduce membrane fluidity due to several characteristics of their head group.[49] In this study, we found that *EPT1*, encoding an enzyme that catalyzes the production of phosphatidylethanolamine[38,50] (Figure 2D), underwent convergent positive selection in the hadal-living YHSC and *P. swirei* (Table S12). Furthermore, many amino acids unique to the YHSC or *P. swirei* were identified (Figure 2E), which suggested that accelerated mutation in the amino acid sequence of EPT1 may be essential to hadal adaptation.

Expansion and positive selection of genes encoding translation initiation factors and ribosomal proteins in the Yap hadal sea cucumbers improved resistance to protein synthesis inhibition

Protein synthesis is the most pressure-sensitive biological process.[4] In prokaryotic organisms, the maximum hydrostatic pressure at which organisms can grow is limited by protein synthesis inhibition.[51] The step that is most inhibited by hydrostatic pressure in protein synthesis is the binding of aminoacyl-tRNA to the ribosome-mRNA complex; this process requires a large increase in volume, which is prevented by high pressure.[4,52,53] High pressure may also lead to ribosome dissociation and further protein synthesis inhibition.[54–56] Protein synthesis inhibition is also aggravated by low temperature.[11,12] Thus, the expansion of genes that promote protein synthesis, bind aminoacyl-tRNA to ribosomes, and maintain the structural integrity of the ribosome may reduce protein synthesis inhibition.

Protein synthesis is mainly regulated at the initiation stage rather than during elongation and termination.[57] At least four gene families, in which the YHSC has more members than other species analyzed were involved in the initiation pathway: eIF4-gamma/eIF5/eIF2-epsilon (W2), middle domain of eukaryotic initiation factor 4G (MIF4G), eukaryotic elongation factor 5A hypusine DNA-binding OB fold (eIF-5A), initiation factor 2 subunit family (IF-2B) (Figure S8). Phylogenetic trees of these gene families identified three expanded genes for translation initiation factors in the YHSC (expansion of both W2 and MIF4G is caused by increased copies of the *eIF4G1*): eukaryotic initiation factor 4 gamma 1 (*eIF4G1*), eIF2B δ subunit (*eIF2Bδ*) and *eIF5A* (Figures 3A-3C). *eIF4G1* encodes a "scaffold" protein that can promote translation initiation by

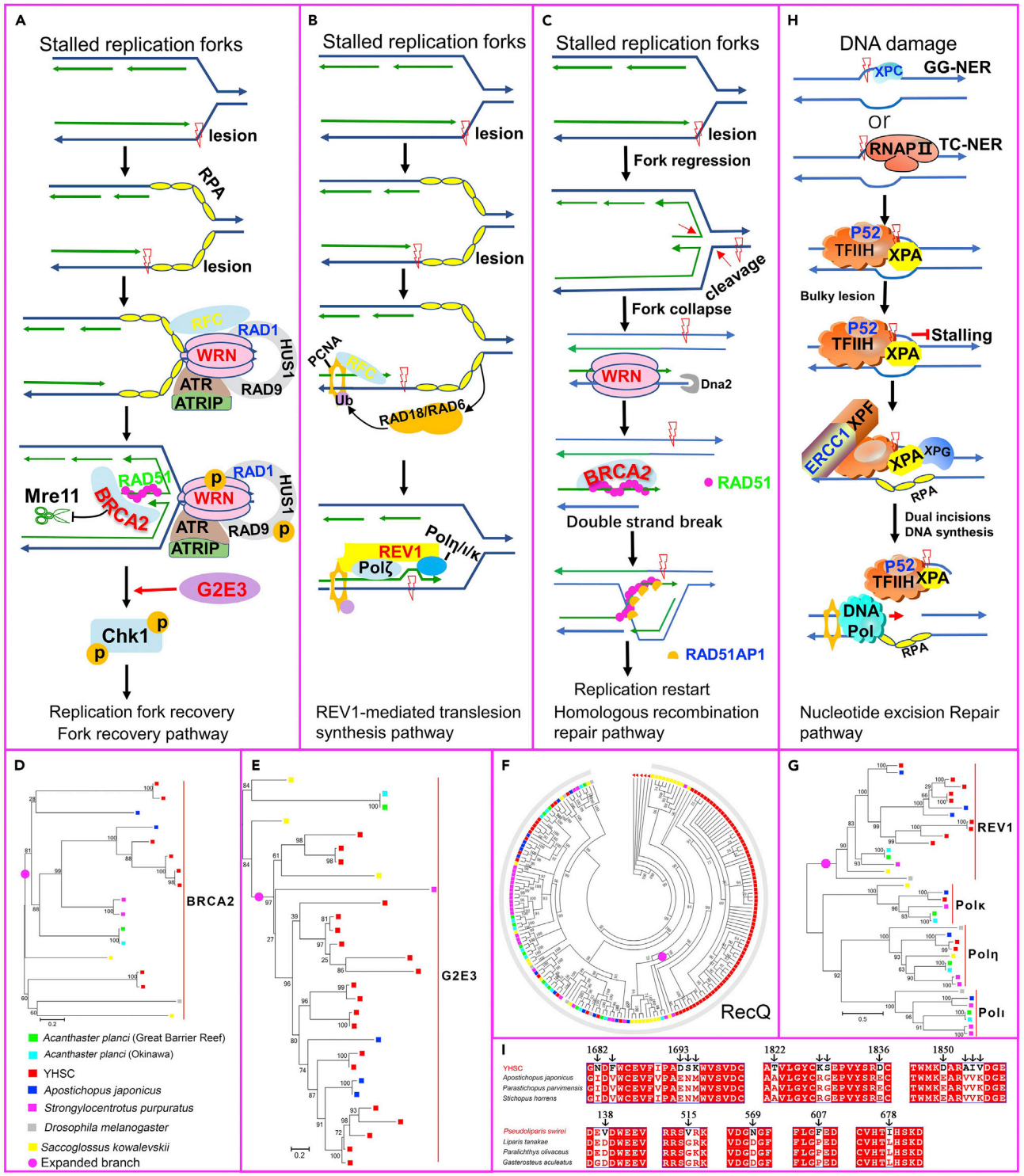

Figure 4. Enhanced DNA protection ability of the YHSC for hadal adaptation

Genes in red and blue underwent the expansion and positive selection in the YHSC, while genes in green and yellow refer to expanded and positively selected genes in *P. swirei*.

(A–C) Mechanisms for restoring stalled and collapsed replication forks.[72,73] Upon encountering obstacles, the replication fork stalled, and the ssDNA is generated and covered by replication protein A (RPA) to avoid secondary structure formation. The stalled fork can be rescued through the fork recovery pathway by activating the downstream effector CHK1[72] (A) or REV1-mediated translesion synthesis[74,75] (B). If the fork is not properly restarted, the replication

Figure 4. *Continued*

fork collapses, one-ended double-strand breaks are induced[76] and the fork is repaired by homologous recombination[72] (C). (A) In the fork recovery pathway, the ssDNA-RPA complex recruits some proteins.[72,77] Meanwhile, BRCA2 catalyzes the formation and stabilization of RAD51-ssDNA filaments, which protects nascent DNA from MRE11-mediated nucleolytic degradation.[69,78] Then, CHK1 is activated with the help of G2E3,[79] and the replication fork restarts after obstacle removal.[69,71] (B) In the translesion synthesis pathway, RAD18 and RAD6 interact with the ssDNA-RPA complex and then ubiquitinate proliferating cell nuclear antigen (PCNA).[80] REV1, which possesses a high affinity for ubiquitinated PCNA, is recruited to lesions and mediates translesion synthesis by interacting with Polζ and one of the three Y-family polymerases (Polι, Polη, and Polκ), and selecting the polymerases required for translesion synthesis.[75,81] (C) In the homologous recombination pathway, the RAD51 filament facilitates strand invasion and homologous recombination after binding with RAD51AP1.[72]

(D) Phylogeny based on proteins containing the BRCA2 repeat domain (*BRCA2*) showed expansion of *BRCA2* in the YHSC genome.

(E) A gene tree of *G2E3* constructed by Orthofinder (version 2.3.8).

(F) Phylogenetic tree based on protein sequences containing DEAD/DEAH box helicases (DEAD). RecQ family labeled with an arc was not further subdivided, as different members could not be distinguished from each other. Nevertheless, 49 genes from the YHSC were annotated as *WRN*, far more than those from other species.

(G) Phylogeny built with proteins containing the impB/mucB/samB family C-terminal domain (IMS_C) showing the expansion of the *REV1* gene.

(H) Nucleotide excision repair pathway. In the presence of DNA lesions, XPC or RNA Pol II loads TFIIH onto DNA, which is promoted by XPA. Upon detection of a bulky lesion, XPF-ERCC1 and XPG make dual incisions.[42]

(I) Multiple sequence alignment of XPC. *XPC* underwent convergent positive selection in the hadal YHSC and *P. swirei*. Amino acids unique to the YHSC or *P. swirei* are indicated by arrows.

binding proteins, including eIF4E, eIF4A, eIF3, and poly(A)-binding protein (PABP)[57,58,63] (Figure 3D). A total of 17 copies of *eIF4G1* were identified in the YHSC genome; in contrast, no more than three copies were identified in any other genome examined (Figure 3A). In deep-sea fish, *eIF4G* is positively selected,[9] indicating that *eIF4G* is involved in deep-sea adaptation. The *eIF2Bδ* gene encodes a subunit of eIF2B, which catalyzes the formation of eIF2·GTP, a rate-limiting step of translation initiation[64,65] (Figure 3D). RNAi inactivation of *eIF2Bδ* decreased global protein synthesis.[65] Four copies of *eIF2Bδ* were found in the YHSC genome, while at most two copies were found in the other genomes examined (Figure 3B). The *eIF5A* gene, previously considered a translation initiation factor, is implicated in the elongation step of protein synthesis and mediates the formation of the first peptide bond[59,62] (Figure 3D). Indeed, the eIF5A protein can increase protein synthesis by 2- to 3-fold in *Saccharomyces cerevisiae*.[59] We identified seven copies of *eIF5A* in the YHSC genome but at most two copies in any other genome examined (Figure 3C). Thus, the expansion of these genes in the translation initiation pathway may increase the synthesis of proteins and reduce protein synthesis inhibition under high pressure and low temperature.

Ribosomal proteins are the major components of ribosomes and function mainly by maintaining ribosome integrity or promoting protein synthesis. In this study, two ribosomal protein genes (*RPS2* and *MRPL4*) underwent expansion, and three mitochondrial ribosomal protein genes (*MRPS27*, *MRPS30,* and *MRPS35*) were positively selected. RPS2, a component of the 40S subunit, mediates the binding of aminoacyl-transfer RNA to the ribosome,[66] a process that is strongly inhibited by high hydrostatic pressure.[53] The YHSC genome harbored 10 copies of the *RPS2* gene, which far exceeded the number of copies in any other genome examined (maximum 2; Figure 3E). MRPL4 maintains the structural integrity of the ribosome and participates in mitochondrial protein translation.[67] There were four copies of the *MRPL4* in the YHSC genome but only one in each of the other genomes examined (Figure 3F). MRPS27, as a small subunit of mitochondrial ribosomes, is required for protein synthesis in mitochondria, and knockdown of *MRPS27* lowered mitochondrial translation.[68] Interestingly, the *MRPS27* was subject to convergent positive selection in the hadal YHSC and *P. swirei* (Table S12), and many amino acids unique to the YHSC or *P. swirei* were identified (Figure 3G), which is suggestive of its important role in hadal adaptation. Thus, the expansion or positive selection of genes for these translation initiation factors and ribosomal proteins may ameliorate protein synthesis inhibition in the hadal zone by increasing protein synthesis, promoting the binding of aminoacyl-tRNA to ribosomes, or improving ribosomal stability.

Yap hadal sea cucumbers exhibited enhanced DNA protection abilities for high-pressure adaptation

Replication forks frequently encounter obstacles, which often lead to fork stalling even under normal conditions.[69,70] Two major strategies are used by cells to rescue stalled forks[71]: replication fork recovery, which involves fork protection, checkpoint activation, removal of replication impediments, and fork resumption[69,72] (Figure 4A), and REV1-mediated translesion synthesis, which uses error-prone translesion-synthesis DNA polymerases to conduct the replication process[74,82] (Figure 4B). When stalled replication forks collapse, producing one-ended double-strand DNA breaks, the collapsed forks are repaired using

homologous recombination[72] (Figure 4C). However, DNA synthesis can be interrupted by high hydrostatic pressure, and the resumption of stalled or collapsed replication forks is also a pressure-sensitive process.[4,8,83] Here, we identified expansions in four genes associated with recovery of stalled replication forks in the YHSC genome, including Breast cancer type 2 (*BRCA2*), Werner syndrome protein (*WRN*), G2/M-phase-specific E3 ubiquitin protein ligase (*G2E3*) and *REV1*. BRCA2 functions in the fork recovery pathway and homologous recombination repair pathway by mediating the assembly of *RAD51* onto *ssDNA* (forming *RAD51* filaments) and stabilizing *RAD51* filaments[84–86] (Figures 4A and 4C). In the fork recovery pathway, the *RAD51* filaments protect nascent DNA at stalled replication forks from MRE11-mediated nucleolytic degradation[69,86–88] (Figure 4A). During homologous recombination repair, *RAD51* filaments promote the invasion and exchange of homologous DNA with the help of RAD51-associated protein 1 (RAD51AP1)[85,89,90] (Figure 4C). There were eight copies of *BRCA2* in the YHSC genome but two at most in any other genome examined (Figure 4D). Furthermore, the *RAD51AP1* was positively selected in the YHSC (Table S15). Interestingly, the genome of a hadal snailfish captured from Yap Trench has more copies of *RAD51* than other teleost genomes analyzed,[15] indicating that the enhanced formation of *RAD51* filaments mediated by *BRCA2* may be essential for hadal adaptation. *G2E3*, the expression of which is induced by DNA damage, participates in replication fork recovery by activating checkpoint kinase 1 (CHK1) kinase[79,91,92] (Figure 4A). We identified 20 copies of *G2E3* in the YHSC genome, compared with three at most in all other genomes examined (Figure 4E). *WRN*, a member of the RecQ family, is a checkpoint protein in the replication fork recovery and double-strand DNA break repair pathway with ATP-dependent 3′-5′ DNA helicase activity[72,77,93] (Figures 4A and 4C). Far more copies of *WRN* were identified in the YHSC genome than in any other genome examined (Figure 4F). Finally, REV1, as a scaffold protein, mediates translesion synthesis by interacting with other translesion synthesis DNA polymerases and selecting the polymerases required for translesion synthesis[75] (Figure 4B). In addition, REV1 also participates in translesion synthesis by employing its dCMP transferase activity, which inserts a dCMP opposite a lesion.[94] The YHSC genome has 9 copies of *REV1*, at least four more than in any other genome examined (Figure 4G). The expansion of genes involved in rescuing stalled or damaged replication forks may provide a solution for DNA synthesis in the hadal zone.

High hydrostatic pressure also leads to DNA damage.[4,6,9] In the YHSC genome, another conspicuous change occurred in the genes in the nucleotide excision repair pathway (Figure 4H). Three genes at least were subjected to positive selection in this pathway: *XPC*, TFIIH basal transcription factor complex p52 subunit (*p52*), and excision repair cross-complementation Group 1 (*ERCC1*). XPC recognizes sites of DNA damage and initiates nucleotide excision repair (*NER*)[42,95] (Figure 4H). In this study, the *XPC* experienced convergent positive selection in the hadal YHSC and *P. swirei* (Table S12), and many YHSC- or *P. swirei*-specific amino acid substitutions were found (Figure 4I), which is suggestive of its important role in hadal adaptation. *p52* and *ercc1* promote the unwinding of DNA around a lesion and excise lesion-containing DNA fragments (Figure 4H). Thus, the expansion and positive selection of genes in replication fork recovery and the nucleotide excision repair pathway may protect DNA from damage exerted by the high pressure in the hadal zone.

Limitations of the study

In this study, we have tried to collect as many echinoderm genomes as possible for comparative analyses. However, only quite a few genomes are available at present. Such, our analyses are limited to the available genomic data, and this situation may be improved accompanying the increased publication of echinoderm genomes.

STAR★METHODS

Detailed methods are provided in the online version of this paper and include the following:

- KEY RESOURCES TABLE
- RESOURCE AVAILABILITY
  - Lead contact
  - Materials availability
  - Data and code availability
- EXPERIMENTAL MODEL AND SUBJECT DETAILS
- METHOD DETAILS
  - Sample collection

- Sequencing and assembly of the YHSC genome
- Elimination of bacterial contamination and redundancy in YHSC genome
- Transcriptome sequencing
- Genome annotation
- Phylogenetic position of the YHSC
- Inference of whole genome duplications from ks distributions
- Evolution of gene families in the YHSC
- Positive selection analysis
- Identification of repeat elements in the YHSC genome
- Fatty acid profiles in phospholipids

- QUANTIFICATION AND STATISTICAL ANALYSIS
- ADDITIONAL RESOURCES

SUPPLEMENTAL INFORMATION

Supplemental information can be found online at https://doi.org/10.1016/j.isci.2022.105545.

ACKNOWLEDGMENTS

This study was supported by the National Program on Key Basic Research Project (973 Program) (2015CB755903), China Agricultural Research System (CARS-47), China Ocean Mineral Resources R & D Association Program (DY135-B2-16), Fujian Science and Technology Department (2021N5008).

AUTHOR CONTRIBUTIONS

Chen, X.H and Zhang, L.S designed this study; Ao, J.Q., Ruan, L.W., and Wang, Y.G., collected the materials. He, T.L, Mu, Y.N., and Mu, PF performed the genome assembly and genome annotation. Gao, Y and Liu, D.G run the software of Orthofinder. The pfam domain in the genome used in the study was identified by Zhang, L.S. The Fatty acid profiles in phospholipids were determined by Lin, X.H. Shao, G.M wrote and revised the article, built all the evolutionary trees and drew all the figures.

DECLARATION OF INTERESTS

The authors declare no competing Interests.

Received: December 12, 2021
Revised: January 18, 2022
Accepted: November 7, 2022
Published: December 22, 2022

REFERENCES

1. Jamieson, A.J. (2015). The Hadal Zone: Life in the Deepest Oceans (Cambridge University Press).

2. Cossins, A.R., and MacDonald, A.G. (1984). Homeoviscous theory under pressure: II. The molecular order of membranes from deep-sea fish. Biochim. Biophys. Acta Biomembr. *776*, 144–150. https://doi.org/10.1016/0005-2736(84)90260-8.

3. Kato, M., and Hayashi, R. (1999). Effects of high pressure on lipids and biomembranes for understanding high-pressure-induced biological phenomena. Biosci. Biotechnol. Biochem. *63*, 1321–1328. https://doi.org/10.1271/bbb.63.1321.

4. Follonier, S., Panke, S., and Zinn, M. (2012). Pressure to kill or pressure to boost: a review on the various effects and applications of hydrostatic pressure in bacterial biotechnology. Appl. Microbiol. Biotechnol. *93*, 1805–1815. https://doi.org/10.1007/s00253-011-3854-6.

5. Schwarz, J.R., and Landau, J.V. (1972). Hydrostatic pressure effects on *Escherichia coli*: site of inhibition of protein synthesis. J. Bacteriol. *109*, 945–948. https://doi.org/10.1128/jb.109.2.945-948.1972.

6. Aertsen, A., and Michiels, C.W. (2005). Mrr instigates the SOS response after high pressure stress in *Escherichia coli*. Mol. Microbiol. *58*, 1381–1391. https://doi.org/10.1111/j.1365-2958.2005.04903.x.

7. Dixon, D.R., Pruski, A.M., and Dixon, L.R.J. (2004). The effects of hydrostatic pressure change on DNA integrity in the hydrothermal-vent mussel *Bathymodiolus azoricus*: implications for future deep-sea mutagenicity studies. Mutat. Res. *552*, 235–246. https://doi.org/10.1016/j.mrfmmm.2004.06.026.

8. Yayanos, A.A., and Pollard, E.C. (1969). A study of the effects of hydrostatic pressure on macromolecular synthesis in *Escherichia coli*. Biophys. J. *9*, 1464–1482. https://doi.org/10.1016/s0006-3495(69)86466-0.

9. Lan, Y., Sun, J., Xu, T., Chen, C., Tian, R., Qiu, J.W., and Qian, P.Y. (2018). De novo transcriptome assembly and positive selection analysis of an individual deep-sea fish. BMC Genomics *19*, 394. https://doi.org/10.1186/s12864-018-4720-z.

10. Quinn, P.J. (1988). Effects of temperature on cell membranes. Symp. Soc. Exp. Biol. *42*, 237–258.

11. Farewell, A., and Neidhardt, F.C. (1998). Effect of temperature on in vivo protein synthetic capacity in *Escherichia coli*. J. Bacteriol. *180*, 4704–4710. https://doi.org/10.1128/jb.180.17.4704-4710.1998.

12. Martegani, E., and Alberghina, L. (1977). Low-temperature restriction of the rate of protein synthesis in *Neurospora crassa*. Exp. Mycol. *1*, 339–351. https://doi.org/10.1016/S0147-5975(77)80009-1.

13. Jamieson, A.J., Fujii, T., Mayor, D.J., Solan, M., and Priede, I.G. (2010). Hadal trenches: the ecology of the deepest places on Earth. Trends Ecol. Evol. *25*, 190–197. https://doi.org/10.1016/j.tree.2009.09.009.

14. Wolff, T. (1970). The concept of the hadal or ultra-abyssal fauna. Deep Sea Research and Oceanographic Abstracts *17*, 983–1003. https://doi.org/10.1016/0011-7471(70)90049-5.

15. Mu, Y., Bian, C., Liu, R., Wang, Y., Shao, G., Li, J., Qiu, Y., He, T., Li, W., Ao, J., et al. (2021). Whole genome sequencing of a snailfish from the Yap Trench (~7, 000 m) clarifies the molecular mechanisms underlying adaptation to the deep sea. PLoS Genet. *17*, e1009530. https://doi.org/10.1371/journal.pgen.1009530.

16. Wang, K., Shen, Y., Yang, Y., Gan, X., Liu, G., Hu, K., Li, Y., Gao, Z., Zhu, L., Yan, G., et al. (2019). Morphology and genome of a snailfish from the Mariana Trench provide insights into deep-sea adaptation. Nat. Ecol. Evol. *3*, 823–833. https://doi.org/10.1038/s41559-019-0864-8.

17. Chu, C., Li, X., and Wu, Y. (2019). GAPPadder: a sensitive approach for closing gaps on draft genomes with short sequence reads. BMC Genomics *20*, 426. https://doi.org/10.1186/s12864-019-5703-4.

18. Liu, B., Shi, Y., Yuan, J., Hu, X., Zhang, H., Li, N., Li, Z., Chen, Y., Mu, D., and Fan, W. (2013). Estimation of genomic characteristics by analyzing k-mer frequency in de novo genome projects. Preprint at arXiv. https://doi.org/10.48550/arXiv.1308.2012.

19. van Berkum, N.L., Lieberman-Aiden, E., Williams, L., Imakaev, M., Gnirke, A., Mirny, L.A., Dekker, J., and Lander, E.S. (2010). Hi-C: a method to study the three-dimensional architecture of genomes. J. Vis. Exp. 1869. https://doi.org/10.3791/1869.

20. Koch, L. (2016). Chicago HighRise for genome scaffolding. Nat. Rev. Genet. *17*, 194. https://doi.org/10.1038/nrg.2016.23.

21. Bocklandt, S., Hastie, A., and Cao, H. (2019). Bionano genome mapping: high-throughput, ultra-long molecule genome analysis system for precision genome assembly and haploid-resolved structural variation discovery. Adv. Exp. Med. Biol. *1129*, 97–118. https://doi.org/10.1007/978-981-13-6037-4_7.

22. Benjamin, A.M., Nichols, M., Burke, T.W., Ginsburg, G.S., and Lucas, J.E. (2014). Comparing reference-based RNA-Seq mapping methods for non-human primate data. BMC Genomics *15*, 570. https://doi.org/10.1186/1471-2164-15-570.

23. Chen, Y., Zhang, Y., Wang, A.Y., Gao, M., and Chong, Z. (2021). Accurate long-read de novo assembly evaluation with Inspector. Genome Biol. *22*, 312. https://doi.org/10.1186/s13059-021-02527-4.

24. Miller, A.K., Kerr, A.M., Paulay, G., Reich, M., Wilson, N.G., Carvajal, J.I., and Rouse, G.W. (2017). Molecular phylogeny of extant Holothuroidea (echinodermata). Mol. Phylogenet. Evol. *111*, 110–131. https://doi.org/10.1016/j.ympev.2017.02.014.

25. Ward, R.D., Holmes, B.H., and O'Hara, T.D. (2008). DNA barcoding discriminates echinoderm species. Mol. Ecol. Resour. *8*, 1202–1211. https://doi.org/10.1111/j.1755-0998.2008.02332.x.

26. Altis, S. (1999). Origin and tectonic evolution of the Caroline Ridge and the Sorol Trough, western tropical Pacific, from admittance and a tectonic modeling analysis. Tectonophysics *313*, 271–292. https://doi.org/10.1016/S0040-1951(99)00204-8.

27. Fujiwara, T., Tamura, C., Nishizawa, A., Fujioka, K., Kobayashi, K., and Iwabuchi, Y. (2000). Morphology and tectonics of the Yap Trench. Mar. Geophys. Res. *21*, 69–86. https://doi.org/10.1023/A:1004781927661.

28. Kobayashi, K. (2004). Origin of the Palau and Yap trench-arc systems. Geophys. J. Int. *157*, 1303–1315. https://doi.org/10.1111/j.1365-246X.2003.02244.x.

29. Lee, S.M. (2004). Deformation from the convergence of oceanic lithosphere into Yap trench and its implications for early-stage subduction. J. Geodyn. *37*, 83–102. https://doi.org/10.1016/j.jog.2003.10.003.

30. Vanneste, K., Van de Peer, Y., and Maere, S. (2013). Inference of genome duplications from age distributions revisited. Mol. Biol. Evol. *30*, 177–190. https://doi.org/10.1093/molbev/mss214.

31. Zwaenepoel, A., and Van de Peer, Y. (2019). wgd-simple command line tools for the analysis of ancient whole-genome duplications. Bioinformatics *35*, 2153–2155. https://doi.org/10.1093/bioinformatics/bty915.

32. Okumura, S.I., Kimura, K., Sakai, M., Waragaya, T., Furukawa, S., Takahashi, A., and Yamamori, K. (2009). Chromosome number and telomere sequence mapping of the Japanese sea cucumber *Apostichopus japonicus*. Fish. Sci. *75*, 249–251. https://doi.org/10.1007/s12562-008-0025-5.

33. Zhang, X., Sun, L., Yuan, J., Sun, Y., Gao, Y., Zhang, L., Li, S., Dai, H., Hamel, J.F., Liu, C., et al. (2017). The sea cucumber genome provides insights into morphological evolution and visceral regeneration. PLoS Biol. *15*, e2003790. https://doi.org/10.1371/journal.pbio.2003790.

34. De Bie, T., Cristianini, N., Demuth, J.P., and Hahn, M.W. (2006). CAFE: a computational tool for the study of gene family evolution. Bioinformatics *22*, 1269–1271. https://doi.org/10.1093/bioinformatics/btl097.

35. Han, M.V., Thomas, G.W.C., Lugo-Martinez, J., and Hahn, M.W. (2013). Estimating gene gain and loss rates in the presence of error in genome assembly and annotation using CAFE 3. Mol. Biol. Evol. *30*, 1987–1997. https://doi.org/10.1093/molbev/mst100.

36. Hall, M.R., Kocot, K.M., Baughman, K.W., Fernandez-Valverde, S.L., Gauthier, M.E.A., Hatleberg, W.L., Krishnan, A., McDougall, C., Motti, C.A., Shoguchi, E., et al. (2017). The crown-of-thorns starfish genome as a guide for biocontrol of this coral reef pest. Nature *544*, 231–234. https://doi.org/10.1038/nature22033.

37. Liao, X., Li, M., Hu, K., Wu, F.X., Gao, X., and Wang, J. (2021). A sensitive repeat identification framework based on short and long reads. Nucleic Acids Res. *49*, e100. https://doi.org/10.1093/nar/gkab563.

38. Ahmed, M.Y., Al-Khayat, A., Al-Murshedi, F., Al-Futaisi, A., Chioza, B.A., Pedro Fernandez-Murray, J., Self, J.E., Salter, C.G., Harlalka, G.V., Rawlins, L.E., et al. (2017). A mutation of EPT1 (SELENOI) underlies a new disorder of Kennedy pathway phospholipid biosynthesis. Brain *140*, 547–554. https://doi.org/10.1093/brain/aww318.

39. Loïodice, I., Alves, A., Rabut, G., Van Overbeek, M., Ellenberg, J., Sibarita, J.B., and Doye, V. (2004). The entire Nup107-160 complex, including three new members, is targeted as one entity to kinetochores in mitosis. Mol. Biol. Cell *15*, 3333–3344. https://doi.org/10.1091/mbc.e03-12-0878.

40. Geng, L., Wang, S., Zhang, F., Xiong, K., Huang, J., Zhao, T., Shi, D., Lv, F., Li, L., Liang, D., et al. (2019). SNX17 (sorting nexin 17) mediates atrial fibrillation onset through endocytic trafficking of the Kv1.5 (potassium voltage-gated channel subfamily A member 5) channel. Circ. Arrhythm. Electrophysiol. *12*, e007097. https://doi.org/10.1161/circep.118.007097.

41. Körner, C., Knauer, R., Stephani, U., Marquardt, T., Lehle, L., and von Figura, K. (1999). Carbohydrate deficient glycoprotein syndrome type IV: deficiency of dolichyl-P-Man:Man(5)GlcNAc(2)-PP-dolichyl mannosyltransferase. EMBO J. *18*, 6816–6822. https://doi.org/10.1093/emboj/18.23.6816.

42. Li, C.L., Golebiowski, F.M., Onishi, Y., Samara, N.L., Sugasawa, K., and Yang, W. (2015). Tripartite DNA lesion recognition and verification by XPC, TFIIH, and XPA in nucleotide excision repair. Mol. Cell *59*, 1025–1034. https://doi.org/10.1016/j.molcel.2015.08.012.

43. Oliver, K.R., and Greene, W.K. (2009). Transposable elements: powerful facilitators of evolution. Bioessays *31*, 703–714. https://doi.org/10.1002/bies.200800219.

44. Chong, P.L., Cossins, A.R., and Weber, G. (1983). A differential polarized phase fluorometric study of the effects of high hydrostatic pressure upon the fluidity of cellular membranes. Biochemistry *22*, 409–415. https://doi.org/10.1021/bi00271a026.

45. Kato, M., Hayashi, R., Tsuda, T., and Taniguchi, K. (2002). High pressure-induced changes of biological membrane. Study on the membrane-bound Na(+)/K(+)-ATPase as a model system. Eur. J. Biochem. *269*, 110–118. https://doi.org/10.1046/j.0014-2956.2002.02621.x.

46. Hashimoto, M., Hossain, S., Yamasaki, H., Yazawa, K., and Masumura, S. (1999). Effects of eicosapentaenoic acid and docosahexaenoic acid on plasma membrane fluidity of aortic endothelial cells. Lipids *34*, 1297–1304. https://doi.org/10.1007/s11745-999-0481-6.

47. Ferdinandusse, S., Denis, S., Mooijer, P.A., Zhang, Z., Reddy, J.K., Spector, A.A., and Wanders, R.J. (2001). Identification of the peroxisomal β-oxidation enzymes involved in the biosynthesis of docosahexaenoic acid. J. Lipid Res. *42*, 1987–1995. https://doi.org/10.1016/S0022-2275(20)31527-3.

48. Van Veldhoven, P.P. (2010). Biochemistry and genetics of inherited disorders of peroxisomal fatty acid metabolism. J. Lipid Res. *51*, 2863–2895. https://doi.org/10.1194/jlr.R005959.

49. Fajardo, V.A., McMeekin, L., and LeBlanc, P.J. (2011). Influence of phospholipid species on membrane fluidity: a meta-analysis for a novel phospholipid fluidity index. J. Membr. Biol. *244*, 97–103. https://doi.org/10.1007/s00232-011-9401-7.

50. Horibata, Y., Elpeleg, O., Eran, A., Hirabayashi, Y., Savitzki, D., Tal, G., Mandel, H., and Sugimoto, H. (2018). EPT1 (selenoprotein I) is critical for the neural development and maintenance of plasmalogen in humans. J. Lipid Res. *59*, 1015–1026. https://doi.org/10.1194/jlr.P081620.

51. Pope, D.H., and Berger, L.R. (1973). Inhibition of metabolism by hydrostatic pressure: what limits microbial growth? Arch. Mikrobiol. *93*, 367–370. https://doi.org/10.1007/bf00427933.

52. Pavlovic, M., Hörmann, S., Vogel, R.F., and Ehrmann, M.A. (2005). Transcriptional response reveals translation machinery as target for high pressure in *Lactobacillus sanfranciscensis*. Arch. Microbiol. *184*, 11–17. https://doi.org/10.1007/s00203-005-0021-4.

53. Schwarz, J.R., and Landau, J.V. (1972). Inhibition of cell-free protein synthesis by hydrostatic pressure. J. Bacteriol. *112*, 1222–1227. https://doi.org/10.1128/jb.112.3.1222-1227.1972.

54. Gross, M., Lehle, K., Jaenicke, R., and Nierhaus, K.H. (1993). Pressure-induced dissociation of ribosomes and elongation cycle intermediates. Stabilizing conditions and identification of the most sensitive functional state. Eur. J. Biochem. *218*, 463–468. https://doi.org/10.1111/j.1432-1033.1993.tb18397.x.

55. Infante, A.A., and Baierlein, R. (1971). Pressure-induced dissociation of sedimenting ribosomes: effect on sedimentation patterns. Proc. Natl. Acad. Sci. USA *68*, 1780–1785. https://doi.org/10.1073/pnas.68.8.1780.

56. Schulz, E., Lüdemann, H.D., and Jaenicke, R. (1976). High pressure equilibrium studies on the dissociation-association of *E. coli* ribosomes. FEBS Lett. *64*, 40–43. https://doi.org/10.1016/0014-5793(76)80243-8.

57. Jackson, R.J., Hellen, C.U.T., and Pestova, T.V. (2010). The mechanism of eukaryotic translation initiation and principles of its regulation. Nat. Rev. Mol. Cell Biol. *11*, 113–127. https://doi.org/10.1038/nrm2838.

58. Prévôt, D., Darlix, J.L., and Ohlmann, T. (2003). Conducting the initiation of protein synthesis: the role of eIF4G. Biol. Cell *95*, 141–156. https://doi.org/10.1016/s0248-4900(03)00031-5.

59. Henderson, A., and Hershey, J.W. (2011). Eukaryotic translation initiation factor (eIF) 5A stimulates protein synthesis in *Saccharomyces cerevisiae*. Proc. Natl. Acad. Sci. USA *108*, 6415–6419. https://doi.org/10.1073/pnas.1008150108.

60. Sasikumar, A.N., Perez, W.B., and Kinzy, T.G. (2012). The many roles of the eukaryotic elongation factor 1 complex. Wiley Interdiscip. Rev. RNA *3*, 543–555. https://doi.org/10.1002/wrna.1118.

61. Tzivelekidis, T., Jank, T., Pohl, C., Schlosser, A., Rospert, S., Knudsen, C.R., Rodnina, M.V., Belyi, Y., and Aktories, K. (2011). Aminoacyl-tRNA-charged eukaryotic elongation factor 1A is the bona fide substrate for *Legionella pneumophila* effector glucosyltransferases. PLoS One *6*, e29525. https://doi.org/10.1371/journal.pone.0029525.

62. Gregio, A.P.B., Cano, V.P.S., Avaca, J.S., Valentini, S.R., and Zanelli, C.F. (2009). eIF5A has a function in the elongation step of translation in yeast. Biochem. Biophys. Res. Commun. *380*, 785–790. https://doi.org/10.1016/j.bbrc.2009.01.148.

63. Costello, J.L., Kershaw, C.J., Castelli, L.M., Talavera, D., Rowe, W., Sims, P.F.G., Ashe, M.P., Grant, C.M., Hubbard, S.J., and Pavitt, G.D. (2017). Dynamic changes in eIF4F-mRNA interactions revealed by global analyses of environmental stress responses. Genome Biol. *18*, 201. https://doi.org/10.1186/s13059-017-1338-4.

64. Pavitt, G.D. (2005). eIF2B, a mediator of general and gene-specific translational control. Biochem. Soc. Trans. *33*, 1487–1492. https://doi.org/10.1042/bst20051487.

65. Tohyama, D., Yamaguchi, A., and Yamashita, T. (2008). Inhibition of a eukaryotic initiation factor (eIF2Bdelta/F11A3.2) during adulthood extends lifespan in *Caenorhabditis elegans*. FASEB J. *22*, 4327–4337. https://doi.org/10.1096/fj.08-112953.

66. Kowalczyk, P., Woszczyński, M., and Ostrowski, J. (2002). Increased expression of ribosomal protein S2 in liver tumors, posthepactomized livers, and proliferating hepatocytes in vitro. Acta Biochim. Pol. *49*, 615–624.

67. Andiappan, A.K., Wang, D.Y., Anantharaman, R., Parate, P.N., Suri, B.K., Low, H.Q., Li, Y., Zhao, W., Castagnoli, P., Liu, J., and Chew, F.T. (2011). Genome-wide association study for atopy and allergic rhinitis in a Singapore Chinese population. PLoS One *6*, e19719. https://doi.org/10.1371/journal.pone.0019719.

68. Davies, S.M.K., Lopez Sanchez, M.I.G., Narsai, R., Shearwood, A.M.J., Razif, M.F.M., Small, I.D., Whelan, J., Rackham, O., and Filipovska, A. (2012). MRPS27 is a pentatricopeptide repeat domain protein required for the translation of mitochondrially encoded proteins. FEBS Lett. *586*, 3555–3561. https://doi.org/10.1016/j.febslet.2012.07.043.

69. Liao, H., Ji, F., Helleday, T., and Ying, S. (2018). Mechanisms for stalled replication fork stabilization: new targets for synthetic lethality strategies in cancer treatments. EMBO Rep. *19*, e46263. https://doi.org/10.15252/embr.201846263.

70. Cox, M.M., Goodman, M.F., Kreuzer, K.N., Sherratt, D.J., Sandler, S.J., and Marians, K.J. (2000). The importance of repairing stalled replication forks. Nature *404*, 37–41. https://doi.org/10.1038/35003501.

71. Zeman, M.K., and Cimprich, K.A. (2014). Causes and consequences of replication stress. Nat. Cell Biol. *16*, 2–9. https://doi.org/10.1038/ncb2897.

72. Ryu, J.S., and Koo, H.S. (2016). Roles of *Caenorhabditis elegans* WRN helicase in DNA damage responses, and a comparison with its mammalian homolog: a mini-review. Gerontology *62*, 296–303. https://doi.org/10.1159/000439200.

73. Yeeles, J.T.P., Poli, J., Marians, K.J., and Pasero, P. (2013). Rescuing stalled or damaged replication forks. Cold Spring Harb. Perspect. Biol. *5*, a012815. https://doi.org/10.1101/cshperspect.a012815.

74. Zhao, L., and Washington, M.T. (2017). Translesion synthesis: insights into the selection and switching of DNA polymerases. Genes *8*, E24. https://doi.org/10.3390/genes8010024.

75. Guo, C., Fischhaber, P.L., Luk-Paszyc, M.J., Masuda, Y., Zhou, J., Kamiya, K., Kisker, C., and Friedberg, E.C. (2003). Mouse Rev1 protein interacts with multiple DNA polymerases involved in translesion DNA synthesis. EMBO J. *22*, 6621–6630. https://doi.org/10.1093/emboj/cdg626.

76. Cortez, D. (2019). Replication-coupled DNA repair. Mol. Cell *74*, 866–876. https://doi.org/10.1016/j.molcel.2019.04.027.

77. Ryu, J.S., and Koo, H.S. (2017). The *Caenorhabditis elegans* WRN helicase promotes double-strand DNA break repair by mediating end resection and checkpoint activation. FEBS Lett. *591*, 2155–2166. https://doi.org/10.1002/1873-3468.12724.

78. Tye, S., Ronson, G.E., and Morris, J.R. (2021). A fork in the road: where homologous recombination and stalled replication fork protection part ways. Semin. Cell Dev. Biol. *113*, 14–26. https://doi.org/10.1016/j.semcdb.2020.07.004.

79. Schmidt, F., Karnitz, L.M., and Dobbelstein, M. (2015). G2E3 attenuating replicative

stress. Aging *7*, 527–528. https://doi.org/10.18632/aging.100784.

80. Sharma, S., Helchowski, C.M., and Canman, C.E. (2013). The roles of DNA polymerase ζ and the Y family DNA polymerases in promoting or preventing genome instability. Mutat. Res. *743–744*, 97–110. https://doi.org/10.1016/j.mrfmmm.2012.11.002.

81. Rizzo, A.A., and Korzhnev, D.M. (2019). The Rev1-Polζ translesion synthesis mutasome: structure, interactions and inhibition. Enzymes *45*, 139–181. https://doi.org/10.1016/bs.enz.2019.07.001.

82. Lehmann, A.R., Niimi, A., Ogi, T., Brown, S., Sabbioneda, S., Wing, J.F., Kannouche, P.L., and Green, C.M. (2007). Translesion synthesis: Y-family polymerases and the polymerase switch. DNA Repair *6*, 891–899. https://doi.org/10.1016/j.dnarep.2007.02.003.

83. Black, S.L., Dawson, A., Ward, F.B., and Allen, R.J. (2013). Genes required for growth at high hydrostatic pressure in *Escherichia coli* K-12 identified by genome-wide screening. PLoS One *8*, e73995. https://doi.org/10.1371/journal.pone.0073995.

84. Chandramouly, G., Willis, N.A., and Scully, R. (2011). A protective role for BRCA2 at stalled replication forks. Breast Cancer Res. *13*, 314. https://doi.org/10.1186/bcr2918.

85. Jensen, R.B., Carreira, A., and Kowalczykowski, S.C. (2010). Purified human BRCA2 stimulates RAD51-mediated recombination. Nature *467*, 678–683. https://doi.org/10.1038/nature09399.

86. Schlacher, K., Christ, N., Siaud, N., Egashira, A., Wu, H., and Jasin, M. (2011). Double-strand break repair-independent role for BRCA2 in blocking stalled replication fork degradation by MRE11. Cell *145*, 529–542. https://doi.org/10.1016/j.cell.2011.03.041.

87. Hashimoto, Y., Ray Chaudhuri, A., Lopes, M., and Costanzo, V. (2010). Rad51 protects nascent DNA from Mre11-dependent degradation and promotes continuous DNA synthesis. Nat. Struct. Mol. Biol. *17*, 1305–1311. https://doi.org/10.1038/nsmb.1927.

88. Ying, S., Hamdy, F.C., and Helleday, T. (2012). Mre11-dependent degradation of stalled DNA replication forks is prevented by BRCA2 and PARP1. Cancer Res. *72*, 2814–2821. https://doi.org/10.1158/0008-5472.Can-11-3417.

89. Bianco, P.R., Tracy, R.B., and Kowalczykowski, S.C. (1998). DNA strand exchange proteins: a biochemical and physical comparison. Front. Biosci. *3*, D570–D603. https://doi.org/10.2741/a304.

90. Pires, E., Sung, P., and Wiese, C. (2017). Role of RAD51AP1 in homologous recombination DNA repair and carcinogenesis. DNA Repair *59*, 76–81. https://doi.org/10.1016/j.dnarep.2017.09.008.

91. Brooks, W.S., Banerjee, S., and Crawford, D.F. (2007). G2E3 is a nucleo-cytoplasmic shuttling protein with DNA damage responsive localization. Exp. Cell Res. *313*, 665–676. https://doi.org/10.1016/j.yexcr.2006.11.020.

92. Schmidt, F., Kunze, M., Loock, A.C., and Dobbelstein, M. (2015). Screening analysis of ubiquitin ligases reveals G2E3 as a potential target for chemosensitizing cancer cells. Oncotarget *6*, 617–632. https://doi.org/10.18632/oncotarget.2710.

93. Lee, S.J., Yook, J.S., Han, S.M., and Koo, H.S. (2004). A Werner syndrome protein homolog affects C. elegans development, growth rate, life span and sensitivity to DNA damage by acting at a DNA damage checkpoint. Development *131*, 2565–2575. https://doi.org/10.1242/dev.01136.

94. Zhou, Y., Wang, J., Zhang, Y., and Wang, Z. (2010). The catalytic function of the Rev1 dCMP transferase is required in a lesion-specific manner for translesion synthesis and base damage-induced mutagenesis. Nucleic Acids Res. *38*, 5036–5046. https://doi.org/10.1093/nar/gkq225.

95. Kusakabe, M., Onishi, Y., Tada, H., Kurihara, F., Kusao, K., Furukawa, M., Iwai, S., Yokoi, M., Sakai, W., and Sugasawa, K. (2019). Mechanism and regulation of DNA damage recognition in nucleotide excision repair. Genes Environ. *41*, 2. https://doi.org/10.1186/s41021-019-0119-6.

96. Buchfink, B., Reuter, K., and Drost, H.G. (2021). Sensitive protein alignments at tree-of-life scale using DIAMOND. Nat. Methods *18*, 366–368. https://doi.org/10.1038/s41592-021-01101-x.

97. Bolger, A.M., Lohse, M., and Usadel, B. (2014). Trimmomatic: a flexible trimmer for Illumina sequence data. Bioinformatics *30*, 2114–2120. https://doi.org/10.1093/bioinformatics/btu170.

98. Vurture, G.W., Sedlazeck, F.J., Nattestad, M., Underwood, C.J., Fang, H., Gurtowski, J., and Schatz, M.C. (2017). GenomeScope: fast reference-free genome profiling from short reads. Bioinformatics *33*, 2202–2204. https://doi.org/10.1093/bioinformatics/btx153.

99. Wessel, P., and Smith, W.H.F. (1998). New, improved version of generic mapping tools released. Eos Trans. AGU. *79*, 579. https://doi.org/10.1029/98EO00426.

100. Zhang, X., Chen, S., Shi, L., Gong, D., Zhang, S., Zhao, Q., Zhan, D., Vasseur, L., Wang, Y., Yu, J., et al. (2021). Haplotype-resolved genome assembly provides insights into evolutionary history of the tea plant *Camellia sinensis*. Nat. Genet. *53*, 1250–1259. https://doi.org/10.1038/s41588-021-00895-y.

101. Koren, S., Walenz, B.P., Berlin, K., Miller, J.R., Bergman, N.H., and Phillippy, A.M. (2017). Canu: scalable and accurate long-read assembly via adaptive k-mer weighting and repeat separation. Genome Res. *27*, 722–736. https://doi.org/10.1101/gr.215087.116.

102. Li, T., Yu, L., Song, B., Song, Y., Li, L., Lin, X., and Lin, S. (2020). Genome improvement and core gene set refinement of *Fugacium kawagutii*. Microorganisms *8*. https://doi.org/10.3390/microorganisms8010102.

103. Ruan, J., and Li, H. (2020). Fast and accurate long-read assembly with wtdbg2. Nat. Methods *17*, 155–158. https://doi.org/10.1038/s41592-019-0669-3.

104. Li, H. (2013). Aligning sequence reads, clone sequences and assembly contigs with BWA-MEM. Preprint at arXiv. https://doi.org/10.48550/arXiv.1303.3997.

105. Vasimuddin, M., Misra, S., Li, H., and Aluru, S. (2019). Efficient architecture-aware acceleration of BWA-MEM for multicore systems. In IEEE Parallel and Distributed Processing Symposium, pp. 314–324. https://doi.org/10.1109/IPDPS.2019.00041.

106. Walker, B.J., Abeel, T., Shea, T., Priest, M., Abouelliel, A., Sakthikumar, S., Cuomo, C.A., Zeng, Q., Wortman, J., Young, S.K., and Earl, A.M. (2014). Pilon: an integrated tool for comprehensive microbial variant detection and genome assembly improvement. PLoS One *9*, e112963. https://doi.org/10.1371/journal.pone.0112963.

107. Li, H., Handsaker, B., Wysoker, A., Fennell, T., Ruan, J., Homer, N., Marth, G., Abecasis, G., and Durbin, R.; 1000 Genome Project Data Processing Subgroup (2009). The sequence alignment/map format and SAMtools. Bioinformatics *25*, 2078–2079. https://doi.org/10.1093/bioinformatics/btp352.

108. Huerta-Cepas, J., Szklarczyk, D., Heller, D., Hernández-Plaza, A., Forslund, S.K., Cook, H., Mende, D.R., Letunic, I., Rattei, T., Jensen, L.J., et al. (2019). eggNOG 5.0: a hierarchical, functionally and phylogenetically annotated orthology resource based on 5090 organisms and 2502 viruses. Nucleic Acids Res. *47*, D309–D314. https://doi.org/10.1093/nar/gky1085.

109. Camacho, C., Coulouris, G., Avagyan, V., Ma, N., Papadopoulos, J., Bealer, K., and Madden, T.L. (2009). BLAST+: architecture and applications. BMC Bioinformatics *10*, 421. https://doi.org/10.1186/1471-2105-10-421.

110. Moriya, Y., Itoh, M., Okuda, S., Yoshizawa, A.C., and Kanehisa, M. (2007). KAAS: an automatic genome annotation and pathway reconstruction server. Nucleic Acids Res. *35*,

W182–W185. https://doi.org/10.1093/nar/gkm321.

111. Zhang, D., Gao, F., Jakovlić, I., Zou, H., Zhang, J., Li, W.X., and Wang, G.T. (2020). PhyloSuite: an integrated and scalable desktop platform for streamlined molecular sequence data management and evolutionary phylogenetics studies. Mol. Ecol. Resour. *20*, 348–355. https://doi.org/10.1111/1755-0998.13096.

112. Katoh, K., and Standley, D.M. (2013). MAFFT multiple sequence alignment software version 7: improvements in performance and usability. Mol. Biol. Evol. *30*, 772–780. https://doi.org/10.1093/molbev/mst010.

113. Kumar, S., Stecher, G., and Tamura, K. (2016). MEGA7: molecular evolutionary genetics analysis version 7.0 for bigger datasets. Mol. Biol. Evol. *33*, 1870–1874. https://doi.org/10.1093/molbev/msw054.

114. Finn, R.D., Coggill, P., Eberhardt, R.Y., Eddy, S.R., Mistry, J., Mitchell, A.L., Potter, S.C., Punta, M., Qureshi, M., Sangrador-Vegas, A., et al. (2016). The Pfam protein families database: towards a more sustainable future. Nucleic Acids Res. *44*, D279–D285. https://doi.org/10.1093/nar/gkv1344.

115. Price, M.N., Dehal, P.S., and Arkin, A.P. (2009). FastTree: computing large minimum evolution trees with profiles instead of a distance matrix. Mol. Biol. Evol. *26*, 1641–1650. https://doi.org/10.1093/molbev/msp077.

116. Emms, D.M., and Kelly, S. (2019). OrthoFinder: phylogenetic orthology inference for comparative genomics. Genome Biol. *20*, 238. https://doi.org/10.1186/s13059-019-1832-y.

117. dos Reis, M., and Yang, Z. (2011). Approximate likelihood calculation on a phylogeny for Bayesian estimation of divergence times. Mol. Biol. Evol. *28*, 2161–2172. https://doi.org/10.1093/molbev/msr045.

118. Grabherr, M.G., Haas, B.J., Yassour, M., Levin, J.Z., Thompson, D.A., Amit, I., Adiconis, X., Fan, L., Raychowdhury, R., Zeng, Q., et al. (2011). Full-length transcriptome assembly from RNA-Seq data without a reference genome. Nat. Biotechnol. *29*, 644–652. https://doi.org/10.1038/nbt.1883.

119. Chen, S., Zhou, Y., Chen, Y., and Gu, J. (2018). fastp: an ultra-fast all-in-one FASTQ preprocessor. Bioinformatics *34*, i884–i890. https://doi.org/10.1093/bioinformatics/bty560.

120. Li, B., and Dewey, C.N. (2011). RSEM: accurate transcript quantification from RNA-Seq data with or without a reference genome. BMC Bioinformatics *12*, 323. https://doi.org/10.1186/1471-2105-12-323.

121. Li, W., and Godzik, A. (2006). Cd-hit: a fast program for clustering and comparing large sets of protein or nucleotide sequences. Bioinformatics *22*, 1658–1659. https://doi.org/10.1093/bioinformatics/btl158.

122. Simão, F.A., Waterhouse, R.M., Ioannidis, P., Kriventseva, E.V., and Zdobnov, E.M. (2015). BUSCO: assessing genome assembly and annotation completeness with single-copy orthologs. Bioinformatics *31*, 3210–3212. https://doi.org/10.1093/bioinformatics/btv351.

123. Haas, B.J., Papanicolaou, A., Yassour, M., Grabherr, M., Blood, P.D., Bowden, J., Couger, M.B., Eccles, D., Li, B., Lieber, M., et al. (2013). De novo transcript sequence reconstruction from RNA-seq using the Trinity platform for reference generation and analysis. Nat. Protoc. *8*, 1494–1512. https://doi.org/10.1038/nprot.2013.084.

124. Smit, A., and Hubley, R. (2008). RepeatModeler Open-1.0. http://www.repeatmasker.org.

125. Smit, A., Hubley, R., and Green, P. (2013). RepeatMasker Open-4.0. http://www.repeatmasker.org.

126. Benson, G. (1999). Tandem repeats finder: a program to analyze DNA sequences. Nucleic Acids Res. *27*, 573–580. https://doi.org/10.1093/nar/27.2.573.

127. Wang, Y., Song, F., Zhu, J., Zhang, S., Yang, Y., Chen, T., Tang, B., Dong, L., Ding, N., Zhang, Q., et al. (2017). GSA: genome sequence archive. Dev. Reprod. Biol. *15*, 14–18. https://doi.org/10.1016/j.gpb.2017.01.001.

128. National Genomics Data Center Members and Partners (2020). Database resources of the national genomics data center in 2020. Nucleic Acids Res. *48*, D24–D33. https://doi.org/10.1093/nar/gkz913.

129. Shao, G., He, T., Mu, Y., Mu, P., Ao, J., Lin, X., Ruan, L., Wang, Y., Gao, Y., Liu, D., et al. (2022). The genome of a hadal sea cucumber reveals novel adaptive strategies to deep-sea environments. Dryad. https://doi.org/10.5061/dryad.z08kprrfs.

130. Amante, C., and Eakins, B.W. (2009). ETOPO1 1 Arc-Minute Global Relief Model : Procedures, Data Sources and Analysis (Department of Commerce, NOAA,National Oceanic and Atmospheric Administration & National Environmental Satellite, Data, and Information Service).

131. Guiglielmoni, N., Houtain, A., Derzelle, A., Van Doninck, K., and Flot, J.F. (2021). Overcoming uncollapsed haplotypes in long-read assemblies of non-model organisms. BMC Bioinformatics *22*, 303. https://doi.org/10.1186/s12859-021-04118-3.

132. Shu, R., Zhang, J., Meng, Q., Zhang, H., Zhou, G., Li, M., Wu, P., Zhao, Y., Chen, C., and Qin, Q. (2020). A new high-quality draft genome assembly of the Chinese cordyceps *Ophiocordyceps sinensis*. Genome Biol. Evol. *12*, 1074–1079. https://doi.org/10.1093/gbe/evaa112.

133. Wang, Y., Li, X.Y., Xu, W.J., Wang, K., Wu, B., Xu, M., Chen, Y., Miao, L.J., Wang, Z.W., Li, Z., et al. (2022). Comparative genome anatomy reveals evolutionary insights into a unique amphitriploid fish. Nat. Ecol. Evol. *6*, 1354–1366. https://doi.org/10.1038/s41559-022-01813-z.

134. Stanke, M., Steinkamp, R., Waack, S., and Morgenstern, B. (2004). AUGUSTUS: a web server for gene finding in eukaryotes. Nucleic Acids Res. *32*, W309–W312. https://doi.org/10.1093/nar/gkh379.

135. Birney, E., and Durbin, R. (2000). Using GeneWise in the *Drosophila* annotation experiment. Genome Res. *10*, 547–548. https://doi.org/10.1101/gr.10.4.547.

136. Ye, J., McGinnis, S., and Madden, T.L. (2006). BLAST: improvements for better sequence analysis. Nucleic Acids Res. *34*, W6–W9. https://doi.org/10.1093/nar/gkl164.

137. Lanfear, R., Frandsen, P.B., Wright, A.M., Senfeld, T., and Calcott, B. (2017). PartitionFinder 2: new methods for selecting partitioned models of evolution for molecular and morphological phylogenetic analyses. Mol. Biol. Evol. *34*, 772–773. https://doi.org/10.1093/molbev/msw260.

138. Huelsenbeck, J.P., and Ronquist, F. (2001). MRBAYES: Bayesian inference of phylogenetic trees. Bioinformatics *17*, 754–755. https://doi.org/10.1093/bioinformatics/17.8.754.

139. Kimura, M. (1980). A simple method for estimating evolutionary rates of base substitutions through comparative studies of nucleotide sequences. J. Mol. Evol. *16*, 111–120. https://doi.org/10.1007/bf01731581.

140. Ao, J., Mu, Y., Xiang, L.X., Fan, D., Feng, M., Zhang, S., Shi, Q., Zhu, L.Y., Li, T., Ding, Y., et al. (2015). Genome sequencing of the perciform fish *Larimichthys crocea* provides insights into molecular and genetic mechanisms of stress adaptation. PLoS Genet. *11*, e1005118. https://doi.org/10.1371/journal.pgen.1005118.

141. Hedges, S.B., Marin, J., Suleski, M., Paymer, M., and Kumar, S. (2015). Tree of life reveals clock-like speciation and diversification. Mol. Biol. Evol. *32*, 835–845. https://doi.org/10.1093/molbev/msv037.

142. Mu, Y., Huo, J., Guan, Y., Fan, D., Xiao, X., Wei, J., Li, Q., Mu, P., Ao, J., and Chen, X. (2018). An improved genome assembly for *Larimichthys crocea* reveals hepcidin gene expansion with diversified regulation and function. Commun. Biol. *1*, 195. https://doi.org/10.1038/s42003-018-0207-3.

143. Yang, Z. (2007). Paml 4: phylogenetic analysis by maximum likelihood. Mol. Biol. Evol. *24*, 1586–1591. https://doi.org/10.1093/molbev/msm088.

144. Benjamini, Y., and Hochberg, Y. (1995). Controlling the false discovery rate: a practical and powerful approach to multiple testing. J. Roy. Stat. Soc. B *57*, 289–300. https://doi.org/10.1111/j.2517-6161.1995.tb02031.x.

145. Lv, W., Lei, Y., Deng, Y., Sun, N., Liu, X., Yang, L., and He, S. (2020). Accelerated evolution and positive selection of rhodopsin in Tibetan loaches living in high altitude. Int. J. Biol. Macromol. *165*, 2598–2606. https://doi.org/10.1016/j.ijbiomac.2020.10.151.

146. Wang, Y., and Yang, L. (2021). Genomic evidence for convergent molecular adaptation in electric fishes. Genome Biol. Evol. *13*, evab038. https://doi.org/10.1093/gbe/evab038.

147. Yang, Y., Wang, L., Han, J., Tang, X., Ma, M., Wang, K., Zhang, X., Ren, Q., Chen, Q., and Qiu, Q. (2015). Comparative transcriptomic analysis revealed adaptation mechanism of *Phrynocephalus erythrurus*, the highest altitude Lizard living in the Qinghai-Tibet Plateau. BMC Evol. Biol. *15*, 101. https://doi.org/10.1186/s12862-015-0371-8.

STAR★METHODS

KEY RESOURCES TABLE

REAGENT or RESOURCE	SOURCE	IDENTIFIER
Biological samples		
Paelopatides sp. Yap	This manuscript	D149; D150; D152
Apostichopus japonicus	This manuscript	N/A
Chemicals, peptides, and recombinant proteins		
TRIzol	Invitrogen	Cat#15596026
Critical commercial assays		
QIAamp DNA Mini Kit	Qiagen	Cat#51306
NEB Next® Ultra DNA Library Prep Kit	NEB	Cat#E7370L
SMRTbell Template Prep Kit 1.0	Pacific Biosciences	Cat#100-259-100
NEBNext Ultra RNA	NEB	Cat#E7770
Deposited data		
Raw sequence data of Paelopatides sp. Yap	This manuscript	GSA: CRA003479
Assembled genome and annotation file of Paelopatides sp. Yap	This manuscript	Mendeley Data: https://doi.org/10.17632/6gn4kf77zm.1
Apostichopus japonicus reference genome	Zhang et al.[33]	http://www.genedatabase.cn/DownLoad_Haishen_20161129.html
Strongylocentrotus purpuratus reference genome	Ensembl	http://ftp.ensemblgenomes.org/pub/release-47/metazoa/fasta/strongylocentrotus_purpuratus/
Acanthaster planci (Okinawa, Japan) reference genome	Hall et al.[36]	https://marinegenomics.oist.jp/cots/viewer/download?project_id=46
Acanthaster planci (the Great Barrier Reef, Australia) reference genome	Hall et al.[36]	https://marinegenomics.oist.jp/cots/viewer/download?project_id=46
Saccoglossus kowalevskii reference genome	NCBI	https://www.ncbi.nlm.nih.gov/genome/?term=Saccoglossus+kowalevskii
Drosophila melanogaster reference genome	Flybase	http://ftp.flybase.net/genomes/Drosophila_melanogaster/dmel_r6.34_FB2020_03/fasta/
Genome and annotation file of *Pseudoliparis swirei*	Wang et al.[16]	https://figshare.com/articles/dataset/Genome_assembly_of_Mariana_hadal_snailfish/9782414
Genome and annotation file of *Liparis tanakae*	Wang et al.[16]	https://figshare.com/articles/dataset/Genome_assembly_of_Mariana_hadal_snailfish/9782414
Genome and annotation file of *Paralichthys olivaceus*	NCBI	https://www.ncbi.nlm.nih.gov/genome/?term=txid8255[orgn]
Genome and annotation file of *Gasterosteus aculeatus*	Ensemble	http://ftp.ensembl.org/pub/release-104/fasta/gasterosteus_aculeatus/
Holothuria leucospilota	NCBI	DRR023763
Parastichopus californicus	NCBI	SRR1695477
Stichopus chloronotus	NCBI	SRR2846098
Synallactes chuni	NCBI	SRR2895367
Parastichopus parvimensis	NCBI	SRR2484238
Stichopus horrens	NCBI	SRR11535195
Software and algorithms		
diamond (version 2.0.14)	Buchfink et al.[96]	https://github.com/bbuchfink/diamond
trimmomatic (version 0.36)	Bolger et al.[97]	https://anaconda.org/bioconda/trimmomatic

(*Continued on next page*)

Continued

REAGENT or RESOURCE	SOURCE	IDENTIFIER
GenomeScope (version 1.0)	Vurture et al.[98]	http://qb.cshl.edu/genomescope/
Generic Mapping Tools (version 6.0)	Wessel and Smith[99]	https://www.generic-mapping-tools.org/download/
Khaper	Zhang et al.[100]	https://github.com/lardo/khaper
Canu (version 1.7)	Koren et al.[101]	https://anaconda.org/bioconda/canu/files?sort=length&version=1.7&sort_order=asc&page=0
GETA (version 1.0)	Li et al.[102]	https://github.com/chenlianfu/geta
wtdbg2 (version 1.0)	Ruan and Li[103]	https://github.com/ruanjue/wtdbg2
bwa-mem (version 0.7.17)	Li[104]	https://github.com/lh3/bwa
bwa-mem2	Vasimuddin et al.[105]	https://github.com/bwa-mem2/bwa-mem2
Pilon (version 1.22)	Walker et al.[106]	https://github.com/broadinstitute/pilon/releases/
samtools (version 1.12)	Li et al.[107]	https://github.com/samtools/samtools
eggno-emapper (version 0.12.7)	Huerta-Cepas et al.[108]	https://github.com/eggnogdb/eggnog-mapper/releases?page=2
Blast (version 2.6.0)	Camacho et al.[109]	https://ftp.ncbi.nlm.nih.gov/blast/executables/blast+/2.6.0/
KASS (version 2.1)	Moriya et al.[110]	https://www.genome.jp/kaas-bin/kaas_main
Phylosuite (version 1.2.1)	Zhang et al.[111]	https://github.com/dongzhang0725/PhyloSuite/releases
mafft (version 7.453)	Katoh and Standley[112]	https://github.com/bioinformatics-polito/LaRA2-mafft
mega (version 7.0)	Kumar et al.[113]	https://www.megasoftware.net/
wgd (version 1.1)	Zwaenepoel and Van de Peer[31]	https://github.com/arzwa/wgd/releases
pfam (version 31.0)	Finn et al.[114]	http://ftp.ebi.ac.uk/pub/databases/Pfam/releases/Pfam31.0/
FastTree (2.1.11)	Price et al.[115]	https://github.com/PavelTorgashov/FastTree
CAFE (version 4.2)	Bie et al.[34]	https://github.com/hahnlab/CAFE/releases
OrthoFinder (version 2.3.8)	Emms and Kelly[116]	https://bioweb.pasteur.fr/packages/pack@OrthoFinder@2.3.8
PAML package (version 4.9)	dos Reis and Yang[117]	https://anaconda.org/bioconda/paml
Trinity (version 2.1.1)	Grabherr et al.[118]	https://github.com/trinityrnaseq/trinityrnaseq
Fastp (version 0.20.1)	Chen et al.[119]	https://github.com/OpenGene/fastp
RSEM (version 1.3.1)	Li and Dewey[120]	https://anaconda.org/bioconda/rsem/files?sort=ndownloads&sort_order=desc&version=1.3.1
CD-HIT-EST (version 4.8.1)	Li and Godzik[121]	https://github.com/weizhongli/cdhit/releases
BUSCO (version 5.3.0)	Simão et al.[122]	https://github.com/WenchaoLin/BUSCO-Mod
Trans-Decoder (version 5.5.0)	Haas et al.[123]	https://anaconda.org/bioconda/transdecoder/files
CallCodeml	Github	https://github.com/byemaxx/callCodeml
RepeatModeler (version 2.0.1)	Smit and Hubley[124]	https://github.com/Dfam-consortium/RepeatModeler/blob/master/RepeatModeler
RepeatMasker (version 4.0.9)	Smit et al.[125]	https://github.com/rmhubley/RepeatMasker
Tandem Repeats Finder (version 4.09)	Benson[126]	https://tandem.bu.edu/trf/trf.download.html
GraphPad Prism (version 5.0)	GraphPad Software, San Diego	https://graphpad-prism.software.informer.com/5.0/
Other		
Codes, bioinformatic program commands, and key intermediate files	This manuscript	Dryad: https://doi.org/10.17632/6gn4kf77zm.1

RESOURCE AVAILABILITY

Lead contact

Further information and requests for resources and reagents should be directed to and will be fulfilled by the lead contact, Xinhua Chen (chenxinhua@tio.org.cn).

Materials availability

This study did not generate new unique reagents.

Data and code availability

- The raw sequence data generated in this paper were deposited in the Genome Sequence Archive (GSA)[127] of the National Genomics Data Center,[128] Beijing Institute of Genomics (China National Center for Bioinformation), Chinese Academy of Sciences, and are publicly available as of the date of publication. Accession numbers are listed in the key resources table. All genome sequence data and annotation files generated in this paper are available at Mendeley Data: https://data.mendeley.com/datasets/6gn4kf77zm/1, and are publicly available as of the date of publication. The DOI is listed in the key resources table. Existing, publicly available data has been used in this study. Their accession numbers or websites have been listed in the key resources table.
- Codes, bioinformatic program commands, and key intermediate files are available via Dryad: https://datadryad.org/stash/share/BATlLeHmrdDiWKzybITl1nATobLm30h8qXbM98yKE4o, and are publicly available as of the date of publication.[129] DOI is listed in the key resources table.
- Any additional information required to reanalyze the data reported in this paper is available from the lead contact upon request.

EXPERIMENTAL MODEL AND SUBJECT DETAILS

This study does not include experiments or subjects.

METHOD DETAILS

Sample collection

The YHSCs were captured in the Yap Trench on 5 June 2017 at 8°3′19′′N, 137°33′6′′E (5,090 m; no. D149), on 9 June 2017 at 8°3′5"N, 137°35′43"E (6,429 m; no. D150), and on 13 June 2017 at 8°1′22"N; 137°50′41"E (6,633 m; no. D152) using the Jiaolong Manned Submarine (Figure 1A and Table S1). Samples were snap frozen in liquid nitrogen, and transported to our laboratory at Fujian Agriculture and Forestry University, Fuzhou, Fujian Province, China. The whole body of each individual was grinded to mix all the tissues together in liquid nitrogen. The tissue homogenate was used for subsequence molecular work. The topographic base map showing the collection sites in the Yap Trench was drawn using Generic Mapping Tools (version 6.0)[99] based on ETOPO1 bathymetric data.[130] We purchased live *A. japonicus* in Qingdao city, Shandong Province, China, in April 2020. The *Paelopatides* sp. 1 and *Paelopatides* sp. 2 were respectively collected on 8 August 2006 in North Pacific (34°39′00"N, 123°5′00"W, 4100 m) and on 4 September 2012 in Gulf of California (26°21′18"N, 110°44′45.6"W, 2733 m).[24]

Sequencing and assembly of the YHSC genome

In this study, the genomic DNA of YHSC no. D152 was sequenced using both single-molecule real-time (SMRT) sequencing with the Pacific Bioscience (PacBio) Sequel platform and Illumina sequencing with an Illumina X Ten instrument. For Illumina sequencing, genomic DNA was first extracted using the QIAamp DNA Mini Kit (Qiagen). Genomic DNA purity and quality were checked using a Nano Photometer Spectrophotometer (Thermo Fisher Scientific) and 1% agarose gel electrophoresis, respectively. Second, DNA fragmentation was performed using an ultrasonic processor. Each insert fragment was approximately 350 bp long. Terminal repair, base A addition, sequence adapter addition, purification, and PCR amplification were performed to prepare a 350-bp library according to the NEB Next® Ultra DNA Library Prep Kit (NEB, USA). After preliminary quantification using Qubit 2.0 (Invitrogen), the library concentration was diluted to 1 ng/μL. Library insert size was verified using an Agilent 2100 (Agilent Technologies), and Q-PCR was performed to ensure that the library concentration was sufficient for sequencing. Then the library was sequenced using an Illumina HiSeq X Ten. Adapter and low-quality reads were filtered by trimmomatic (version 0.36)[97] with parameters "TruSeq3-PE.fa:2:30:10 LEADING:3 TRAILING:3 SLIDINGWINDOW:4:15 MINLEN:51". The clean reads were used for estimation of genome size, repeat content and heterozygosity rate by using GenomeScope (version 1.0) with k-mer = 21.[98]

For PacBio sequencing, genomic DNA was firstly extracted by using the QIAamp DNA Mini Kit (QiaGen) and assessed by using an Agilent 4200 Bioanalyzer (Agilent Technologies) and agarose gel electrophoresis. Then G-Tubes (Covaris) and AMPure PB magnetic beads were respectively used to shear 8 μg of

extracted DNA and concentrate the DNA fragments. SMRTbell libraries were constructed using SMRTbell Template Prep Kit 1.0 (Pacific Biosciences). The BluePippin system was used to select molecules ≥10 kb in the constructed libraries (Pacific Biosciences). The SMRTbell libraries were sequenced using a Pacific Bioscience Sequel platform. The raw data were cleaned by removing adaptor sequences, polymerase reads with length ≤50 bp, and reads with quality scores ≤0.8. Canu (version 1.7)[101] was used to correct errors in the subreads. Considering the high heterozygosity rate of YHSC genome, wtdbg2 (version 1.0), which did not produce obvious artifactual duplications,[103,131] was used to assemble the subreads into contigs. Then bwa-mem (version 0.7.17)[104] algorithm was used to map the Illumina clean reads against the contigs, and variants that were considered as sequencing errors were polished using Pilon (version 1.22)[106] with default parameters. Finally, the quality of the assembly was evaluated by mapping the Illumina reads to the polished contigs by bwa-mem2.[105] The mapping rate (Mapped reads divided by total reads) was computed by samtools (version 1.12).[107] We also evaluated genome integrity by BUSCO (version 5.3.0) with eukaryota_odb10 database.

Elimination of bacterial contamination and redundancy in YHSC genome

The exclusion of bacterial contamination started with the identification of contigs containing bacterial proteins. First, the non-redundant bacterial and deuterostome proteins were retrieved from the NCBI nr database. Then diamond (version 2.0.14)[96] was used to query each of YHSC proteins against the bacterial and deuterostome proteins with an E-value threshold of 1e-5. Taxonomy assignment for each query sequence was based on the best hits. Exactly, in each best match, the query sequence was assigned to bacteria if the corresponding subject was bacterial, while assigned to YHSC if the subject was from deuterostome proteins. The contigs with ≥50% bacterial proteins or no deuterostome proteins were considered as bacterial sequences and were excluded. Khaper[100] was employed to identify and remove redundant sequences from YHSC genome based on the 209.1 Gb Illumina clean reads with k-mer = 17.

Transcriptome sequencing

The methods of transcriptome sequencing were as follows. Total RNA was extracted from the YHSC using TRIzol (Invitrogen). mRNA was purified from the total RNA using poly-T oligo-attached magnetic beads. Sequencing libraries were generated using NEBNext Ultra RNA (NEB). Briefly, first strand cDNA was synthesized using a random hexamer primer and RNase H. Second strand cDNA synthesis was subsequently performed using buffer, dNTPs, DNA polymerase I and RNase H. The terminal repair, addition of A-tailing and adapter were implemented according to the manual. The libraries were sequenced on an Illumina NovaSeq 6000, and 150 bp paired-end reads were generated. The raw data were cleaned by excluding adaptor sequences and low-quality reads by using Trimmomatic (version 0.36) with parameters "TruSeq3-PE.fa:2:30:10 LEADING:3 TRAILING:3 SLIDINGWINDOW:4:15 MINLEN:51".

Genome annotation

Coding genes in the YHSC genome were predicted by using GETA (version 1.0) pipeline (https://github.com/chenlianfu/geta), which incorporates homology-based predictions, *ab initio* gene predictions, and transcript evidence according to previous reports.[102,132] Exactly, we first built a customized library of repetitive sequences in this genome by RepeatModeler program (version 2.1). This library was further subject to RepeatMasker (version 4.0.7) program to predict a full set of repetitive sequences and also generated a repeat-masked genome with repetitive sequences replaced with Ns. Then RNA-seq reads were trimmed and cleaned using Trimomatic program and aligned against the genome by HiSat2 (version 2.1.0)[133] with default parameters. Transcripts were extracted based on the BAM alignments by the sam2transfrag program implanted in the GETA pipeline. And ORFs were predicted by Trans-Decoder (https://github.com/TransDecoder/TransDecoder). We next applied the AUGUSTUS (version 3.2.2) program[134] to iteratively train gene models using the high-quality transcripts aforementioned. In addition, the homology-based annotation was performed based on the alignment of homolgous proteins from *A. japonicus*, *S. purpuratus*, *A. planci*, *S. kowalevskii*, *Helobdella robusta*, and *branchiostoma floridae* to YHSC genome using TBLASTN in NCBI-Blast+ (version 2.6.0),[109] followed by prediction of exact gene structures by using Gene-Wise (version 2.4.1)[135] based on the blast hits. The final gene set was incorporated by paraCombineGeneModels program in the GETA pipeline. The settings for those tools refer to the "conf_for_big_genome.txt" file, at "https://github.com/chenlianfu/geta/blob/master/conf_for_big_genome.txt". The functions of putative protein-coding genes were annotated by using eggno-emapper (version 0.12.7),[108] which integrates information from both precomputed orthologous groups and phylogenies in the eggnog

database,[108] and also annotated by diamond (version 2.6.0) against the nr database. The KEGG Automatic Annotation Server (KASS) (version 2.1)[110] was used to identify pathway information.

Phylogenetic position of the YHSC

To determine the phylogenetic placement of the YHSC, the barcode regions of three nuclear genes (*18S rRNA*, *28S rRNA*, and *H3*) and two mitochondrial genes (*16S rRNA* and *COI*) in the YHSC genome were used to query the NCBI nt database using BLASTn.[136] Next, available *18S rRNA*, *28S rRNA*, *H3*, *16S rRNA*, and *COI* sequences for extant Holothuroidea were downloaded from GenBank (Table S9). Multigene phylogenies of extant Holothuroidea, including the YHSC, were then reconstructed based on the three nuclear genes or the two mitochondrial genes using Phylosuite (version 1.2.1).[111] In detail, the nucleotide sequences of each gene from all species were aligned using mafft (version 7.453).[112] The aligned sequences of the three nuclear genes were concatenated using the "Concatenate Sequence" program in Phylosuite, as were those of the two mitochondrial genes. The best-fit partitioning schemes and models of evolution were selected based on the results of partitionFinder2[137] in Phylosuite, and phylogenies were inferred using MrBayes[138] in Phylosuite with default settings. Phylogenetic clusters were identified based on a recent revision of the extant Holothuroidea.[24]

The divergence between the YHSC and the seven species that are most closely related to the YHSC in the *Paelopatides, Bathyplotes, and Apostichopus* according to Figure 1B was calculated based on the COI barcode sequences using the model of Kimura 2-parameter distance (K2P)[139] in mega (version 7.0)[113] as previously reported.[25] The COI barcodes of YHSC *Paelopatides sp.* 1, *Paelopatides sp.* 2, *A. japonicus*, *Apostichopus californicus*, *Apostichopus parvimensis*, *Bathyplotes sp.* 1, and *Bathyplotes sp.* 2 (GenBank accession numbers are given in Table S9) were first aligned by the muscle program in mega (version 7.0).[113] Then, the aligned sequences were used to calculate genetic divergence between the YHSC and seven other species using K2P.[139]

Inference of whole genome duplications from ks distributions

Whole genome duplication in YHSC genome was inferred from the whole paranome *Ks* distributions for *A. japonicus* and YHSC together with the *Ks* distribution of their one-to-one orthologs by using wgd (version 1.1).[31] Firstly, the *Ks* distributions of paralogous gene families and one-to-one orthologs were performed by "wgd dmd" and "wgd ksd" commands. The "bokeh serve & wgd viz -i -ks" commands were used to interactively visualize the *Ks* distributions of the paralogous gene families and the *Ks* distributions of one-to-one orthologs together.

Evolution of gene families in the YHSC

Although we attempted to collect genomic data for species closely related to the YHSC, a lack of appropriate data meant that we were limited to four echinoderm genomes: *A. japonicus*, *S. purpuratus*, and two geographically separated populations of *A. planci* (Okinawa, Japan and the Great Barrier Reef, Australia). We also included two additional invertebrate genomes: *D. melanogaster and S. kowalevskii* (sequence sources given in the key resources table).

Functional domains in the protein sequences from the seven genomes were annotated using pfam (version 31.0)[114] with default parameters, which uses the HMM scanning method to classify gene families. We compared domain numbers across the species analyzed. We considered domains with z scores >1.96 and more than 5 members in the YHSC genome to be expanded ones, following Wang et al.[16] To identify expanded genes in expanded domains, protein sequences with the same domain of interest were aligned using mafft (version 7.453),[112] and the resulting alignment was used for phylogenetic tree construction by FastTree (2.1.11)[115] with default parameters. Genes with a z scores >1.96 and no less than 4 copies in YHSC genome were regarded as expanded ones.

Additionally, CAFE (version 4.2)[34,35,140] was used to evaluate the expansion and contraction of gene families in the YHSC genome compared with the other six genomes. CAFE infers the most likely the size of gene families at all internal nodes and identifies gene families with an accelerated rate of gain or loss using the size of gene families and an ultrametric tree as inputs.[34] This analysis had four main steps. First, gene numbers in gene families across the seven genomes were calculated, and a species tree was constructed using OrthoFinder (version 2.3.8)[116] with a "-m msa" parameter. Gene families with $\geq$200 members in any single species were excluded from further analysis.[16] Second, an ultrametric tree was constructed using

MCMCTree in the PAML package (version 4.9)[117], and three soft calibration bounds were set based on timetree[141]: *A. planci-A. japonicus:* 450–605 Ma; *S. purpuratus-S. kowalevskii:* 535–763 Ma; and *A. japonicus-D. melanogaster:* 643–850 Ma. Third, CAFE (version 4.2)[34,35] was used to identify gene families with accelerated rates of gain and loss. Gene families for which the p value of the YHSC branch was <0.01 were defined as significantly expanded or contracted, following a previous study.[142] Fourth, the numbers of gene families that had undergone expansions or contractions were plotted on the phylogenetic tree following a previous study.[34]

Positive selection analysis

Due to the lack of genomic data of Holothuroidea, we attempted to include transcriptome data from this taxon in PSG identification in the YHSC genome. First, we conducted *de novo* assembly and functional annotation of the transcriptome from 6 species (as much as we could collect), including *Holothuria leucospilota* (NCBI Accession: DRR023763), *Parastichopus californicus* (SRR1695477), *Stichopus chloronotus* (SRR2846098), *Synallactes chuni* (SRR2895367), *P. parvimensis* (SRR2484238) and *Stichopus horrens* (SRR11535195) according to previous methods.[9] Briefly, Fastp (version 0.20.1)[119] was used to remove adaptors and low-quality reads. The clean reads were utilized for *de novo* assembly by Trinity (version 2.1.1).[118] RSEM (version 1.3.1)[120] was performed to quantify the transcripts, and only the isoform for a gene with the highest abundance was retained. CD-HIT-EST (version 4.8.1)[121] was employed to remove transcripts with a similarity over 95%, and transcripts less than 200 bp were also excluded from further analysis. BUSCO (version 5.3.0, metazoa_odb10)[122] was used to evaluate the completeness of the transcripts. Species with a complete BUSCO less than 90% were excluded, which means that only *P. parvimensis* and *Stichopus horrens* were used for further analysis (Table S16). Trans-Decoder (version 5.5.0)[123] was used to predict coding regions by integrating the results of a BLAST search against the SWISS-PROT database and a Pfam search against the PFAM-A database into coding region selection.

Considering the completeness of the assembled transcripts, we selected transcripts from *P. parvimensis*, *Stichopus horrens*, YHSC and *A. japonicus* (Table S16) for PSG identification in the YHSC. Briefly, single-copy orthologs and phylogenetic relationships of the four species were inferred by OrthoFinder (version 2.3.8).[116] The single-copy orthologs were aligned by ParaAT (version 2.0) with the "-g" and "-m mafft" options. CallCodeml (https://github.com/byemaxx/callCodeml), which calls Codeml[143] to calculate positive selection in the site-branch model in bulk and to determine the p value with the chi-squared test, was used to calculate the selection pressure of the "foreground" phylogeny (YHSC branch). The p values were corrected by multiple testing correction.[144] Genes with a corrected p value < 0.05 and with Bayesian empirical Bayes (BEB) sites >0.9 were considered PSGs. To study the convergent sequence evolution for hadal adaptation, we also calculated the selection pressure of *P. swirei* in the Mariana Trench using *P. swirei* as the foreground phylogeny and three closely related shallow-sea species according to a previous report,[16] including *P. olivaceus*, *G. aculeatus* and *Liparis tanakae*, as the background phylogeny. The downloaded website of their genome and annotation file are shown in the key resources table. The methods were the same as those for PSG identification in the YHSC genome. The same gene that underwent positive selection in both of the two distantly related taxa was considered as convergent evolution, referring to previous reports.[145–147]

Identification of repeat elements in the YHSC genome

We compared the abundance of repeated elements in the YHSC genome with those in another four echinoderm genomes namely *A. japonicus*, *S. purpuratus*, *A. planci* (Okinawa), *A. planci* (Great Barrier Reef). *De novo* prediction was used to identify repeat elements in these genomes. First, a custom library of transposable elements was constructed for each species using the RepeatModeler pipeline (version 2.01).[124] Repeats were then predicted based on the libraries using RepeatMasker (version 4.1.0).[125] Tandem repeats were predicted using Tandem Repeats Finder (version 4.0.9).[126]

Fatty acid profiles in phospholipids

To explore adaptive changes in cell membrane components in response to increased hydrostatic pressure, various fatty acids (C6–C24) in phospholipids from the three YHSCs (D149, D150, and D152) and six *A. japonicus* were analyzed using gas chromatography-mass spectrometry (GC-MS). Due to sample deficiency, each individual was only measured once.

QUANTIFICATION AND STATISTICAL ANALYSIS

Significant differences in the relative abundance of each fatty acid between the YHSC and *A. japonicus* were identified by using a two-tailed t test as implemented in Microsoft Excel 2019. p values < 0.05 were considered significant. Graphical representations of the data were designed using GraphPad Prism 5.0. Data were presented as the means $\pm$ SEM. The threshold setting for the diamond program was E-value < 1e-5. The cutoff for expanded domains was z scores >1.96 and >5 members in the YHSC genome,[16] while the cutoff for expanded genes was z scores >1.96 and $\geq$4 copies in YHSC genome. For PSG identification, genes with a corrected p value < 0.05 and Bayesian empirical Bayes (BEB) sites >0.9 were considered PSGs. The changes of gene families were inferred by cafe, the ones with p value of the YHSC branch <0.01 were defined as significantly expanded or contracted gene families, following the previous study.[34]

ADDITIONAL RESOURCES

This study does not include additional resources.